International Journal of Nutrology
(Official Journal of the ABRAN - Brazilian Association of Nutrology)

ORIGINAL ARTICLE

DOI: 10.54448/ijn26314

Stratified lipidomic, inflammatory, and oxidative-stress phenotyping of *Helicobacter pylori* infection: study group distinguishing CagA- positive strains in Iraqi adult

Zainab Hudhi Farhood[1,*]

[1] University of Thi-Qar. College of Education for Pure Sciences. Department of Biology, Thi-Qar, Iraq.

*Corresponding author: Zainab Hudhi Farhood.
University of Thi-Qar. College of Education for Pure Sciences. Department of Biology, Thi-Qar, Iraq.
E-mail: zainabhadhi.bio@utq.edu.iq
DOI: https://doi.org/10.54448/ijn26314
Received: 01-10-2026; Revised: 02-20-2026; Accepted: 02-24-2026; Published: 07-23-2026; IJN-id: e26314

Editor: Dr. Idiberto José Zotarelli-Filho, MSc, Ph.D., Post-Doctoral.

Abstract

Introduction: *Helicobacter pylori* is increasingly implicated in extragastric metabolic and atherogenic disease, but human data integrating advanced lipidomics, oxidative-stress biology, and high-density lipoprotein (HDL) functional assessment in a CagA-stratified design remain scarce, particularly in the Middle East. **Objective:** To characterize variations in lipid metabolism across stages of *H. pylori* exposure, distinguishing virulent CagA-positive strains, and to identify the biological pathways mediating this relationship. **Methods.** In this STROBE-compliant case–control study (Al-Nasiriyah General/Turkish Hospital, Dhi Qar, Iraq; September 2025–February 2026), 230 adults aged 18–60 years were assigned to four pre-specified groups: *H. pylori*-naïve controls (n=60), past *H. pylori* exposure (n=50), active CagA-negative infection (n=60), and active CagA-positive infection (n=60), based on ^{13}C-urea breath testing, stool antigen testing, and anti-*H. pylori*/anti-CagA serology. Conventional and advanced lipoproteins, apolipoproteins, atherogenic indices, inflammatory cytokines, oxidative-stress and antioxidant markers, HDL-functional enzymes, adipokines, insulin axis, one-carbon biomarkers, and an untargeted serum lipidomic panel were measured. Multivariable linear regression, ROC analysis with bootstrap-validated LASSO modeling, and bootstrap mediation analyses were performed. **Results:** A monotonic gradient (Control → Past-HP → CagA− → CagA+) was observed for atherogenic, inflammatory, and oxidative biomarkers, with reciprocal declines in apolipoprotein A-I, paraoxonase-1, lecithin– cholesterol acyltransferase, adiponectin, and antioxidant capacity. After adjustment for age, sex, BMI, smoking, diet, physical activity, and inflammation, CagA+ infection was independently associated with elevated oxidized LDL, ApoB/ApoA-I ratio, atherogenic index of plasma, and reduced PON1 activity (all $P<0.001$). Lipidomics revealed elevated saturated ceramides and lyso-phosphatidylcholines with depleted sphingosine-1-phosphate. Oxidative-stress index and inflammation partially mediated the *H. pylori*–lipid associations. **Conclusion:** *H. pylori* infection, particularly with CagA+ strains, is independently associated with an adverse lipid metabolic, lipidomic, and HDL-functional phenotype mediated in part by inflammation and oxidative stress.

Keywords: *Helicobacter pylori*. CagA virulence factor. Dyslipidemia. Oxidized LDL. Paraoxonase-1. Lipidomics. Ceramides. Oxidative stress. Cardiovascular risk.

Graphical Abstract

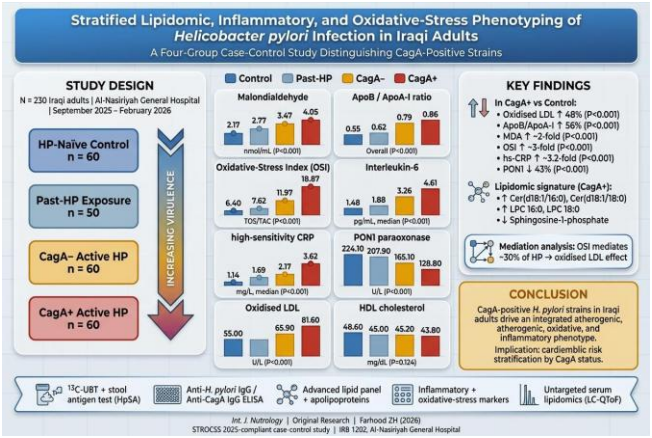

Source: Own authorship.

Introduction

Helicobacter pylori is one of the most prevalent chronic bacterial infections in humans, colonising approximately 43% of the global adult population in the period 2015-2022, with a substantially higher burden in low- and middle-income regions **[1,2]**. The Middle East and North Africa region, including Iraq, continues to carry one of the heaviest burdens; Iraqi adult prevalence estimates range from approximately 47% to 75% across published surveys, and recent multicentre data from Kurdistan and central Iraq report active infection in roughly half of dyspeptic outpatients **[3-5]**. Beyond its established causal role in chronic gastritis, peptic ulcer disease, gastric MALT lymphoma, and non-cardia gastric adenocarcinoma, increasing evidence implicates *H. pylori* in extragastric disorders, including dyslipidaemia, atherosclerotic cardiovascular disease, insulin resistance, and metabolic syndrome **[6-9]**.

The vacuolating cytotoxin A (VacA) and cytotoxin-associated gene A (CagA) products are the most extensively characterised *H. pylori* virulence determinants. The cagA gene, located on the cag pathogenicity island, encodes an oncoprotein translocated into host cells through a type-IV secretion system, where tyrosine phosphorylation engages SHP-2 phosphatase, RUNX3, β-catenin, and NF-κB signalling, driving sustained epithelial inflammation and reactive-oxygen-species (ROS) generation **[10-12]**. Approximately 60% of regional *H. pylori* strains are CagA-positive, and recent Iraqi molecular surveys confirm a comparable prevalence among local clinical isolates **[5,13]**. Importantly, CagA seropositivity rather than *H. pylori* exposure per se has been linked to a 58% greater pooled cardiovascular risk **[7]** and to direct endothelial dysfunction in mechanistic studies showing exosome-mediated ROS formation confined to CagA-positive infection **[14]**.

Several biological pathways have been proposed to connect *H. pylori* with atherogenic dyslipidaemia. First, sustained low-grade systemic inflammation, indexed by interleukin-6 (IL-6), tumour necrosis factor-α (TNF-α), and high-sensitivity C-reactive protein (hs-CRP), can suppress hepatic apolipoprotein A-I (ApoA-I) synthesis and induce hepatic acute-phase secretion of triglyceride-rich lipoproteins **[15-17]**. Second, *H. pylori*-driven oxidative stress, reflected by elevated malondialdehyde (MDA), 4-hydroxynonenal, F_2-isoprostanes, and Total Oxidant Status, with reciprocal depletion of glutathione, paraoxonase-1 (PON1), and Total Antioxidant Capacity, promotes LDL oxidation and HDL functional dysfunction **[18-22]**. Third, the infection impairs cobalamin and folate absorption, raising homocysteine and producing endothelial injury **[23-25]**. Fourth, *H. pylori* modulates adipokine signalling—lowering adiponectin and elevating resistin— and can suppress gastric ghrelin secretion, exacerbating insulin resistance **[9,26,27]**.

Recent advances in plasma lipidomics have shown that selected lipid species—particularly the saturated ceramide Cer(d18:1/16:0), several lyso-phosphatidylcholines, and the sphingolipid mediator sphingosine-1-phosphate (S1P)—are robust independent predictors of cardiovascular events that capture lipid biology not visible in conventional panels **[28-32]**. Whether *H. pylori* infection in general, and CagA-positive infection in particular, induces this proatherogenic lipidomic signature in humans remains incompletely characterised. Iraqi data on *H. pylori* and lipid metabolism are limited: existing reports describe modest lipid alterations in obese Iraqi women with *H. pylori* infection **[33]**, elevated IL-6 and TNF-α in Iraqi seropositive adults **[16]**, and the histopathological correlates of CagA-positive strains **[34]**, but no Iraqi study to date has integrated conventional and advanced lipid panels, apolipoproteins, atherogenic indices, inflammatory and oxidative-stress biomarkers, HDL-functional enzymes, adipokines, the insulin axis, one-carbon biomarkers, and untargeted lipidomics within a single CagA-stratified design.

The present author therefore conducted a STROBE-compliant case-control study at Al-Nasiriyah General/Turkish Hospital with the following pre-specified aims: (i) to characterise lipid metabolic phenotypes across four stages of *H. pylori* exposure-naïve, past, active CagA-negative, and active CagA-positive—using both conventional and advanced lipid panels and an integrated panel of inflammatory, oxidative-stress, HDL-functional, adipokine, insulin-axis, and one-carbon biomarkers; (ii) to define the lipidomic signature, if any, distinguishing CagA-positive infection from controls using untargeted serum lipidomics; (iii) to evaluate the diagnostic discrimination of single biomarkers and a composite multi-marker panel; and (iv) to test, by bootstrap mediation analyses, whether systemic inflammation, oxidative stress, and insulin resistance mediate the relationship between *H. pylori* infection and atherogenic lipid phenotypes.

Materials and Methods

Study design and setting

This was a single-centre, hospital-based, age- and sex-balanced case–control study conducted in accordance with the Strengthening the Reporting of Observational Studies in Epidemiology (STROBE)

statement for cross-sectional and case–control designs **[35]**. Recruitment, sample collection, and laboratory analyses were performed at Al-Nasiriyah General/Turkish Hospital, Dhi Qar Governorate, southern Iraq, from September 2025 through February 2026.

Ethics statement

The study protocol was reviewed and approved by the Institutional Review Board of Al-Nasiriyah General/Turkish Hospital (approval number 1202; date of approval 22 February 2026), and was conducted in accordance with the Declaration of Helsinki, as revised in 2013. Written informed consent was obtained from every participant before any study procedure. All data were de-identified, coded, and stored on a password-protected server accessible only to the named investigators.

Participants and group definitions

Adult outpatients aged 18–60 years presenting to the Gastroenterology and General Internal Medicine clinics with mild–moderate dyspeptic symptoms or for routine evaluation were screened for eligibility. Inclusion criteria were: age 18–60 years, fasting glucose <126 mg/dL, glycated haemoglobin <6.5%, estimated glomerular filtration rate ≥60 mL/min/1.73 m² (CKD-EPI 2021), and normal thyroid function. Exclusion criteria were: established diabetes mellitus, current use of lipid-lowering or antihypertensive medication, advanced liver, kidney, or cardiovascular disease, recent (within 4 weeks) systemic antibiotic, bismuth, or proton-pump-inhibitor exposure, pregnancy or lactation, autoimmune disease, malignancy, and any acute febrile illness within 4 weeks. After post-enrolment exclusions for diagnostic disagreement (UBT–HpSA discordance), incomplete sampling, or withdrawal, 230 participants completed the protocol and were assigned to four pre-specified mutually exclusive groups (Figure 1):

- HP-Naïve Control (n=60): ^{13}C-urea breath test (UBT) negative, *H. pylori* stool antigen (HpSA) negative, and anti-*H. pylori* IgG negative.
- Past-HP exposure (n=50): anti-*H. pylori* IgG positive but UBT and HpSA both negative, with no history of recent eradication therapy.
- CagA-negative Active HP (n=60): UBT and HpSA both positive, anti-CagA IgG negative.
- CagA-positive Active HP (n=60): UBT and HpSA both positive, anti-CagA IgG positive.

Sample-size calculation

Sample size was estimated a priori for the primary outcome (atherogenic index of plasma) using G*Power version 3.1.9.7 (Faul et al., 2007) for an F-test (one-way fixed-effects ANOVA, omnibus) across four independent groups. Based on the effect sizes reported in prior regional case– control data on *H. pylori* and lipid parameters **[33,36]**, and the four-group oxidative-stress gradient observed by Tsukanov and colleagues, a medium effect size of Cohen's f = 0.25 was assumed (Cohen, 1988). With α = 0.05 (two-sided), statistical power (1−β) = 0.80, and number of groups = 4, the minimum total sample size required was n = 180 (45 per group). To allow for approximately 20% post-enrolment loss (diagnostic disagreement, incomplete sampling, withdrawal) and to enhance power for the secondary advanced-lipidomic and mediation analyses, 230 participants were enrolled across the four groups (n=60 HP-Naïve Control, n=50 Past-HP, n=60 CagA– Active HP, n=60 CagA+ Active HP). Sensitivity analyses showed that this final sample size provided > 95% power to detect a medium effect at α = 0.05 and > 80% power to detect a small-to-medium effect (f = 0.20) for all primary lipid, inflammatory, and oxidative-stress outcomes.

H. pylori diagnostic algorithm

Active *H. pylori* status was confirmed by simultaneous positivity on two independent noninvasive tests. The ^{13}C-urea breath test was performed using the Helicobacter Test INFAI® (INFAI GmbH, Bochum, Germany), with delta-over-baseline (DOB) values measured by infrared isotope-selective spectrometry on a POCone analyser (Otsuka Pharmaceutical, Tokyo, Japan); DOB ≥4‰ defined positivity. The *H. pylori* stool antigen test was performed by enzyme-linked immunosorbent assay (Premier Platinum HpSA PLUS; Meridian Bioscience, Cincinnati, OH, USA), with optical density ratio ≥0.140 defining positivity. Anti-*H. pylori* IgG, anti-CagA IgG, and anti-VacA IgG were quantified by validated commercial ELISA kits (Demeditec Diagnostics GmbH, Kiel, Germany; catalogue numbers DE3454, DE3461, and DE3471, respectively), supplied locally through authorised regional distributors. All samples were assayed in duplicate, with intra- and inter-assay coefficients of variation maintained below 8% and 10%, respectively.

Clinical, anthropometric, and lifestyle assessments

All participants underwent a structured clinical interview by a trained physician, using a pre-piloted Arabic-language case-record form. Height and weight were measured to the nearest 0.1 cm and 0.1 kg, respectively, using a calibrated stadiometer and

electronic scale; body mass index (BMI) was calculated as weight (kg)/height (m)². Waist and hip circumferences were measured to the nearest 0.5 cm using a non-elastic anthropometric tape. Blood pressure was measured in triplicate after 5 minutes of seated rest using a validated automated oscillometric device (Omron M3 Comfort, Omron Healthcare, Kyoto, Japan), and the mean of the second and third readings was recorded. Gastrointestinal symptoms were assessed using the Gastrointestinal Symptom Rating Scale (GSRS) **[37]**. Mediterranean diet adherence was quantified by the 14-item Mediterranean Diet Adherence Screener (MEDAS) **[38]**, adapted for Iraqi food culture. Habitual physical activity was measured by the Arabic version of the long-form International Physical Activity Questionnaire (IPAQ) **[39]**, with energy expenditure expressed as metabolic-equivalent-task minutes per week (MET-min/week).

Sample collection and processing

After at least 12 hours of overnight fasting, venous blood was drawn between 08:00 and 10:00 a.m. via antecubital venepuncture into ethylenediaminetetraacetic acid (EDTA)-coated tubes, sodium fluoride/potassium oxalate tubes (for fasting glucose), and plain serum-separator tubes (BD Vacutainer®, Becton Dickinson, Plymouth, UK). Serum was obtained after clot retraction at room temperature for 30 minutes followed by centrifugation at 3000 ×g for 10 minutes at 4 °C. Aliquots were transferred to cryovials and stored at −80 °C in a continuously monitored biofreezer (Thermo Scientific Forma 88000 series, Thermo Fisher Scientific, Waltham, MA, USA) until analysis. Freeze–thaw cycles were limited to a single occurrence per aliquot.

Routine biochemistry and conventional lipid panel

Fasting plasma glucose, total cholesterol, triglycerides, HDL cholesterol, directly measured LDL cholesterol, alanine aminotransferase, aspartate aminotransferase, alkaline phosphatase, gamma-glutamyl transferase, total bilirubin, albumin, urea, creatinine, calcium, and uric acid were measured on a Roche Cobas® c501 modular automated chemistry analyser (Roche Diagnostics, Mannheim, Germany), using the manufacturer's reagent cassettes and following ISO 15189-aligned internal quality-control protocols. Directly measured LDL cholesterol was determined by a homogeneous direct assay (Roche Direct LDL-C plus 3rd Generation; Cobas reagent), and Friedewald-calculated values were retained for cross-validation **[40]**; Friedewald and direct LDL agreed within ±5% in 96% of subjects. Glycated haemoglobin (HbA1c) was measured by ion-exchange high-performance liquid chromatography (Bio-Rad D-10™, Bio-Rad Laboratories, Hercules, CA, USA), standardised to the IFCC reference method. Erythrocyte sedimentation rate was measured by the modified Westergren method on an Alifax TEST 1® analyser (Alifax, Polverara, Italy). Complete blood counts were performed on a Sysmex XN-550 haematology analyser (Sysmex Corporation, Kobe, Japan). Thyroid function (TSH, free T4) was measured by electrochemiluminescence immunoassay on a Roche Cobas e411 platform. Estimated glomerular filtration rate was calculated using the 2021 CKD-EPI creatinine equation **[41]**.

Advanced lipoproteins and apolipoproteins

Small dense LDL cholesterol (sdLDL-C) was measured by a homogeneous direct assay (sdLDL-EX 'SEIKEN'; Randox Laboratories, Crumlin, UK; catalogue SD3717) on the Cobas c501 platform **[42]**. Lipoprotein(a) was measured by an isoform-insensitive immunoturbidimetric method (Randox LP3437) and reported in nmol/L. Oxidized LDL was measured by ELISA (Mercodia Oxidized LDL ELISA, catalogue 10-1143-01; Mercodia AB, Uppsala, Sweden) **[43]**. Apolipoproteins A-I, A-II, B, C-III, and E were quantified by immunoturbidimetric assays (Randox apolipoprotein kits) on the Cobas c501. Remnant-cholesterol was calculated as [total cholesterol − HDL-C − directly measured LDL-C].

Inflammatory cytokines

High-sensitivity C-reactive protein was measured by particle-enhanced immunoturbidimetric assay (Roche Tina-quant® C-Reactive Protein Gen.3 high-sensitive) on the Cobas c501. Serum interleukin-6, interleukin-8, interleukin-1β, and tumour necrosis factor-α were measured by sandwich ELISA (Elabscience Biotechnology, Houston, TX, USA; catalogue numbers E-EL-H6156, E-EL-H0048, E-EL-H0149, and E-EL-H0109, respectively), with absorbance read at 450 nm on a BioTek ELx800 microplate reader (BioTek Instruments, Winooski, VT, USA). All samples were assayed in duplicate; intra- and inter-assay coefficients of variation were below 7% and 9%.

Oxidative-stress and antioxidant markers

Total Antioxidant Capacity (TAC) and Total Oxidant Status (TOS) were measured by the colorimetric methods of Erel using the corresponding ready-to-use kits from Rel Assay Diagnostics (Mega Tıp Sanayi, Gaziantep, Türkiye) **[44,45]**. The Oxidative Stress Index (OSI) was calculated as the ratio

TOS/TAC, expressed as an arbitrary unit. Malondialdehyde was determined by the thiobarbituric-acid-reactive substances (TBARS) method (Cayman Chemical TBARS Assay 10009055; Cayman Chemical, Ann Arbor, MI, USA). 4-Hydroxynonenal was quantified by competitive ELISA (OxiSelect HNE Adduct Competitive ELISA STA-838; Cell Biolabs, San Diego, CA, USA). F_2-isoprostanes (8-iso-prostaglandin F2α) were measured by enzyme immunoassay (Cayman 8-Isoprostane EIA 516351). Reduced glutathione was measured by enzymatic recycling (Cayman GSH/GSSG Ratio Detection Kit 703002). Superoxide dismutase activity was measured by the xanthine oxidase–WST-1 method (Cayman SOD 706002), and catalase activity by formaldehyde-based colorimetry (Cayman Catalase 707002).

HDL-functional enzymes

Paraoxonase-1 paraoxonase activity (against the substrate paraoxon) and arylesterase activity (against phenyl acetate) were measured spectrophotometrically using the standardised Rel Assay Diagnostics PON1 paraoxonase and arylesterase kits (catalogue numbers RL0047 and RL0048), as previously described **[21]**. Lecithin–cholesterol acyltransferase activity was measured by a fluorescent self-quenching substrate assay (Roar Biomedical LCAT Activity Assay; Roar Biomedical, New York, NY, USA), and cholesteryl ester transfer protein activity by the corresponding fluorescent assay (Roar Biomedical CETP Activity Assay).

Adipokines, insulin axis, and one-carbon biomarkers

Serum leptin, adiponectin, resistin, and total ghrelin were measured by commercial sandwich

ELISAs (BioVendor Research and Diagnostic Products, Brno, Czech Republic; catalogue numbers RD194002100, RD195023100, RD191016100, and RD194062400R). Fasting insulin was measured by ELISA (Mercodia Iso-Insulin 10-1113-01). HOMA-IR was calculated as [fasting insulin (μU/mL) × fasting glucose (mg/dL)]/405; QUICKI was calculated as 1/[log(insulin) + log(glucose)]. Total plasma homocysteine was measured by chemiluminescence microparticle immunoassay on an Abbott Architect i2000SR platform; serum vitamin B12 and folate were measured by electrochemiluminescence on a Cobas e411 analyser.

Untargeted serum lipidomics

Serum lipids were extracted from 50-μL aliquots using a modified Folch method (chloroform:methanol 2:1 v/v) **[46]**, with addition of deuterated SPLASH® LIPIDOMIX internal standards (Avanti Polar Lipids, Alabaster, AL, USA) prior to extraction. Untargeted lipidomic profiling was performed at a regional accredited core facility on an Agilent 6546 LC/Q-TOF system coupled to an Agilent 1290 Infinity II UHPLC (Agilent Technologies, Santa Clara, CA, USA), using a reversed-phase Waters Acquity BEH C18 column (2.1 × 100 mm, 1.7 μm). Data were acquired in both positive and negative ion modes. Pooled quality-control samples were injected every 10 study samples. Lipid identification used the LIPID MAPS database and MS-DIAL/LipidBlast spectral libraries; annotations were retained at LIPID MAPS Confidence Level 2. Peak areas were normalised to internal standards and to total ion current. The lipidomic data matrix was $\log_2$-transformed and Pareto-scaled prior to multivariate analysis **[47]**.

Atherogenic indices

The Atherogenic Index of Plasma (AIP) was computed as $\log_{10}$(TG/HDL-C), with values >0.21 indicating elevated cardiovascular risk per Dobiásová and Frohlich **[48]**. Castelli risk indices I and II were calculated as TC/HDL-C and LDL-C/HDL-C, respectively. The Atherogenic Coefficient and TG/HDL ratio were derived from standard formulae. The Triglyceride–Glucose (TyG) index was calculated as ln**[(TG × glucose)/2]**. The ApoB/ApoA-I ratio was computed directly from measured apolipoproteins.

Statistical analysis

Continuous variables were assessed for normality by the Shapiro–Wilk test. Normally distributed variables are presented as mean ± SD and compared across the four groups by one-way ANOVA; non-normally distributed variables are presented as median (IQR) and compared by the Kruskal–Wallis test. Categorical variables are presented as n (%) and compared by Pearson χ^2 or Fisher exact test. Pre-specified pairwise contrasts were assessed by Mann–Whitney U or Tukey HSD with Bonferroni adjustment. Spearman rank correlations with Benjamini–Hochberg FDR correction described biomarker associations. Multivariable linear regression estimated independent associations of *H. pylori* group with each lipid outcome adjusted for age, sex, BMI, current smoking, MEDAS, log-physical-activity, and log-hs-CRP; all variance inflation factors were below 3. Diagnostic performance was evaluated by ROC analysis with DeLong 95% confidence intervals **[49]** and Youden-optimised cut-offs **[50]**. A composite biomarker panel was developed by L1-penalised (LASSO) logistic regression with 10-fold cross-validation **[51]**. Bootstrap mediation analyses with

1,000 nonparametric resamples were conducted following Preacher and Hayes **[52]**. Untargeted lipidomic data were analysed in MetaboAnalyst v5.0 **[47]**. Analyses used R version 4.3.1 (glmnet, pROC, cutpointr, randomForest, mediation packages). Two-sided P-values <0.05 were considered statistically significant.

Results

Participant characteristics

Of 412 outpatient attendees screened, 142 were excluded for failing eligibility criteria, 40 for diagnostic disagreement or incomplete sampling, leaving 230 participants who completed the protocol and were distributed across the four pre-specified groups (Figure 1). Demographic, anthropometric, clinical, and lifestyle characteristics are summarised in Table 1. The four groups were broadly comparable in sex distribution, residence, blood pressure, heart rate, diet quality, and smoking pattern, with modest but statistically significant differences in age (37.6 ± 10.4 years in HP-Naïve controls versus 43.1 ± 9.3 years in CagA+ subjects, p=0.030), education (p<0.001), BMI (27.1 ± 4.1 vs 29.3 ± 4.5 kg/m², P=0.017), waist circumference (p=0.022), and physical activity (median 2,068 vs 1,496 MET-min/week, p<0.001). The Gastrointestinal Symptom Rating Scale (GSRS) total score and symptom duration showed expected monotonic increases with infection status (both P<0.001). These observed imbalances informed adjustment for age, sex, BMI, smoking, MEDAS, log-IPAQ, and log-hs-CRP in subsequent multivariable analyses.

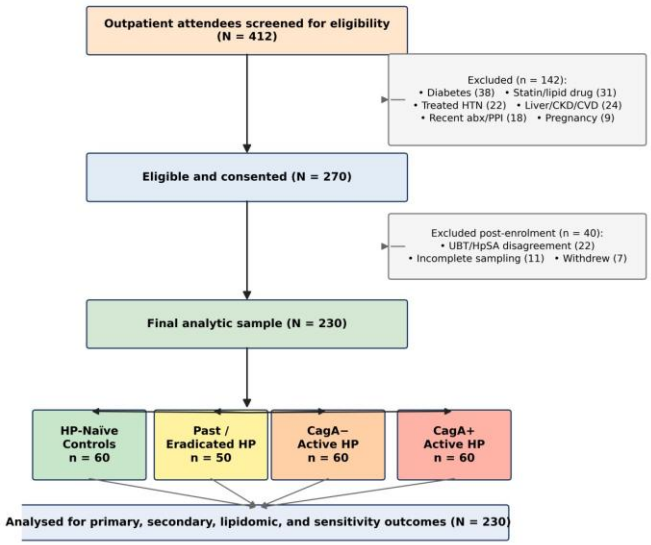

Figure 1. STROBE flow diagram of participant recruitment and group allocation. Of 412 outpatient attendees screened, 142 were excluded for failing eligibility criteria (diabetes, lipid-lowering or antihypertensive medications, advanced liver/kidney/cardiovascular disease, recent antibiotic or proton-pump-inhibitor exposure, or pregnancy). After post-enrolment exclusion of 40 participants for diagnostic disagreement (UBT and HpSA discordant), incomplete sampling, or withdrawal, 230 participants completed the protocol and contributed to all analyses, distributed across four pre-specified groups. UBT, ^{13}C-urea breath test; HpSA, *H. pylori* stool antigen test; abx, antibiotics; PPI, proton-pump inhibitor; HTN, hypertension; CKD, chronic kidney disease; CVD, cardiovascular disease. Source: Own authorship.

Table 1. Demographic, anthropometric, clinical, and lifestyle characteristics of the study population by group (N = 230).

Variables	HP-Naïve Control (n = 60)	Past-HP (n = 50)	CagA− Active HP (n = 60)	CagA+ Active HP (n = 60)	p value
Demographics					
Age (years)	37.6 ± 10.4	41.0 ± 11.3	41.2 ± 10.1	43.1 ± 9.3	0.030
Education (years)	13.7 ± 3.2	11.1 ± 4.1	11.1 ± 3.2	11.1 ± 3.6	<0.001
Female, n (%)	33 (55.0)	27 (54.0)	35 (58.3)	26 (43.3)	0.386
Urban, n (%)	31 (51.7)	31 (62.0)	32 (53.3)	34 (56.7)	0.767
Anthropometrics					
BMI (kg/m²)	27.1 ± 4.1	27.4 ± 4.4	27.3 ± 3.8	29.3 ± 4.5	0.017
Waist circumference (cm)	88.1 ± 7.6	89.5 ± 8.7	88.5 ± 7.5	92.3 ± 8.3	0.022
Waist-to-hip ratio	0.88 ± 0.05	0.88 ± 0.04	0.88 ± 0.05	0.89 ± 0.05	0.430
Vital signs					
Systolic BP (mmHg)	121.0 ± 10.0	123.5 ± 11.8	121.5 ± 10.3	122.9 ± 10.9	0.588
Diastolic BP (mmHg)	74.2 ± 7.6	75.3 ± 9.4	77.2 ± 8.4	76.5 ± 7.4	0.204
Heart rate (bpm)	76.6 ± 9.8	75.0 ± 9.5	78.5 ± 7.9	75.5 ± 8.6	0.160
Lifestyle					
Current smoker, n (%)	11 (18.3)	6 (12.0)	11 (18.3)	15 (25.0)	—
Pack-years among smokers	0.0 (0.0–0.7)	0.0 (0.0–0.0)	0.0 (0.0–1.2)	0.0 (0.0–7.2)	0.079
Shisha (sessions/week)	0.0 (0.0–0.0)	0.0 (0.0–0.0)	0.0 (0.0–0.0)	0.0 (0.0–0.0)	0.351
MEDAS score (0–14)	6.7 ± 2.1	6.7 ± 2.2	6.7 ± 1.9	6.6 ± 2.4	0.983
Daily fat intake (g/day)	81.5 ± 21.0	84.3 ± 22.5	82.7 ± 20.6	85.1 ± 24.6	0.806
Physical activity (MET-min/week)	2068 (1505–3220)	1598 (1085–2384)	1428 (1040–2024)	1496 (1151–1860)	<0.001
Symptoms					
GSRS total score	4.2 (2.2–6.0)	7.0 (5.1–8.9)	10.1 (8.8–12.0)	11.0 (9.4–13.0)	<0.001
Symptom duration (months)	0.9 (0.3–1.6)	9.0 (6.4–12.8)	11.9 (6.7–16.5)	11.9 (5.8–16.8)	<0.001
Family history, n (%)					
H. pylori	28 (46.7)	17 (34.0)	25 (41.7)	26 (43.3)	0.595
Dyslipidemia	17 (28.3)	13 (26.0)	25 (41.7)	12 (20.0)	0.064
Premature CVD	11 (18.3)	9 (18.0)	13 (21.7)	5 (8.3)	0.232
Gastric cancer	2 (3.3)	1 (2.0)	2 (3.3)	2 (3.3)	—

Continuous variables are presented as mean ± SD (normally distributed) or median (Q1–Q3) (non-normal); categorical variables as n (%). P values from one-way ANOVA, Kruskal–Wallis test, or Pearson χ^2 (or Fisher exact). Group definitions: HP-Naïve Control = UBT, HpSA, and anti-*H. pylori* IgG all negative; Past-HP = anti-*H. pylori* IgG positive but UBT and HpSA negative; CagA− Active HP = UBT/HpSA positive with anti-CagA IgG negative; CagA+ Active HP = UBT/HpSA positive with anti-CagA IgG positive. **Abbreviations:** BMI, body mass index; BP, blood pressure; bpm, beats per minute; CVD, cardiovascular disease; GSRS, Gastrointestinal Symptom Rating Scale; IPAQ, International Physical Activity Questionnaire; MEDAS, Mediterranean Diet Adherence Screener; MET, metabolic equivalent task. Source: Own authorship.

H. pylori diagnostic markers and routine biochemistry

As expected by design, the four groups exhibited highly significant separation across all *H. pylori* diagnostic markers (all p<0.001; Table 2). UBT delta-over-baseline rose from a median of 0.74‰ in HP-Naïve controls to 13.17‰ in CagA+ subjects, and the stool antigen optical-density ratio increased approximately 8-fold across active-infection groups. Anti-*H. pylori* IgG was sharply elevated in all *H. pylori*-exposed subjects, while anti-CagA and anti-VacA IgG showed the largest fold-changes specifically in the CagA+ group (anti-CagA IgG median 36.0 vs 3.0 U/mL in controls, p<0.001), confirming serological differentiation of CagA-positive strains. Routine haematology, glycaemic indices, hepatic and renal function, and thyroid-function indices were comparable across groups, consistent with the eligibility criteria; however, the erythrocyte sedimentation rate (ESR) increased monotonically across the infection gradient (median 8 mm/h in controls vs 18 mm/h in CagA+ subjects, p<0.001), providing an independent, low-tech corroboration of the systemic inflammatory burden linked to *H. pylori* activity.

Table 2. *Helicobacter pylori* diagnostic markers and routine biochemistry by study group.

Variables	HP-Naïve Control (n = 60)	Past-HP (n = 50)	CagA− Active HP (n = 60)	CagA+ Active HP (n = 60)	p value
H. pylori diagnostics					
UBT delta-over-baseline (‰)	0.74 (0.44–1.12)	1.48 (0.80–2.49)	11.39 (6.29–15.30)	13.17 (9.43–21.91)	<0.001
Stool antigen test (OD ratio)	0.061 (0.037–0.095)	0.071 (0.043–0.098)	0.490 (0.414–0.586)	0.518 (0.386–0.682)	<0.001
Anti-*H. pylori* IgG (U/mL)	4.0 (2.9–5.5)	30.9 (24.1–37.1)	52.8 (42.0–70.6)	53.9 (43.2–69.0)	<0.001
Anti-CagA IgG (U/mL)	3.0 (2.4–4.3)	7.6 (4.2–11.7)	3.7 (2.6–4.7)	36.0 (19.4–52.5)	<0.001
Anti-VacA IgG (U/mL)	2.8 (1.7–3.9)	9.9 (6.7–14.5)	6.9 (3.5–10.3)	31.2 (20.8–39.4)	<0.001
Hematology					
WBC (×10⁹/L)	6.63 ± 1.73	6.65 ± 1.30	7.10 ± 1.68	7.04 ± 1.61	0.237
Hemoglobin (g/dL)	13.6 ± 1.7	13.5 ± 1.5	13.0 ± 1.8	13.1 ± 1.4	0.091
Platelets (×10⁹/L)	270 ± 55	267 ± 59	258 ± 54	255 ± 55	0.396
ESR (mm/hr)	8 (6–11)	12 (10–18)	14 (10–18)	18 (14–24)	<0.001
Glycemic					
Fasting glucose (mg/dL)	94.1 ± 8.5	94.0 ± 8.4	92.9 ± 9.0	92.5 ± 7.6	0.671
HbA1c (%)	5.48 ± 0.33	5.44 ± 0.29	5.53 ± 0.30	5.48 ± 0.34	0.498
Liver function					
ALT (U/L)	20 (18–30)	20 (17–28)	22 (19–28)	22 (17–25)	0.546
AST (U/L)	20 (16–24)	20 (15–22)	19 (16–25)	19 (17–23)	0.661
ALP (U/L)	78 ± 19	80 ± 19	84 ± 23	75 ± 23	0.103
GGT (U/L)	20 (14–31)	23 (16–34)	22 (17–30)	22 (17–28)	0.678
Albumin (g/dL)	4.26 ± 0.27	4.28 ± 0.29	4.38 ± 0.34	4.30 ± 0.25	0.096
Total bilirubin (mg/dL)	0.67 (0.57–0.80)	0.69 (0.56–0.84)	0.70 (0.55–0.83)	0.71 (0.58–0.92)	0.586
Renal function					
Urea (mg/dL)	28.5 ± 7.2	28.1 ± 5.9	26.5 ± 8.2	28.8 ± 6.8	0.291
Creatinine (mg/dL)	0.84 ± 0.15	0.85 ± 0.17	0.83 ± 0.16	0.89 ± 0.17	0.143
eGFR (mL/min/1.73 m²)	100.2 ± 12.4	99.7 ± 13.5	99.8 ± 15.0	97.7 ± 12.4	0.728
Thyroid function					
TSH (mIU/L)	2.09 (1.65–2.90)	1.87 (1.47–2.27)	1.92 (1.50–2.42)	1.79 (1.39–2.32)	0.097
Free T4 (ng/dL)	1.17 ± 0.19	1.20 ± 0.19	1.22 ± 0.20	1.21 ± 0.20	0.404

Continuous variables are presented as mean ± SD (normal) or median (Q1–Q3) (non-normal). P values from one-way ANOVA or Kruskal–Wallis. All participants met the eligibility criteria for fasting glucose <126 mg/dL, HbA1c <6.5%, eGFR ≥60 mL/min/1.73 m², and normal thyroid function. **Abbreviations:** ALP, alkaline phosphatase; ALT, alanine aminotransferase; AST, aspartate aminotransferase; eGFR, estimated glomerular filtration rate (CKD-EPI 2021); ESR, erythrocyte sedimentation rate; GGT, gamma-glutamyl transferase; HbA1c, glycated haemoglobin; HpSA, *H. pylori* stool antigen test; OD, optical density; T4, thyroxine; TSH, thyroid-stimulating hormone; UBT, ¹³C-urea breath test; WBC, white blood cell count. Source: Own authorship.

Conventional and advanced lipid profile

The lipid phenotype shifted progressively from HP-Naïve controls to CagA+ subjects (Table 3). Total cholesterol (175.2 ± 27.8 → 194.2 ± 28.9 mg/dL, p=0.007), triglycerides (median 111.5 → 153.0 mg/dL, p=0.016), LDL-C (110.8 ± 28.0 → 125.9 ± 28.2 mg/dL, p=0.014), VLDL-C (P=0.017), and non-HDL-C (126.5 ± 28.5 → 150.4 ± 29.2 mg/dL, p<0.001) all increased across the gradient, whereas HDL-C declined modestly without reaching unadjusted significance (48.6 ± 11.0 → 43.8 ± 11.4 mg/dL, P=0.124). Among advanced lipoproteins, small-dense LDL cholesterol rose by 53% from controls to CagA+ subjects (23.5 ± 8.8 → 35.9 ± 12.5 mg/dL, p<0.001), and oxidised LDL increased by 48% (55.0 ± 17.9 → 81.6 ± 15.3 U/L, P<0.001). Lipoprotein(a) did not differ across groups (p=0.733). Apolipoprotein analyses revealed reciprocal shifts: ApoA-I declined progressively (156.0 ± 23.4 → 126.8 ± 24.4 mg/dL, p<0.001), while ApoB rose (84.4 ± 18.7 → 105.3 ± 23.5 mg/dL, p<0.001), producing a 56% rise in the ApoB/ApoA-I ratio (0.55 ± 0.15 → 0.86 ± 0.27, p<0.001). All atherogenic indices—Atherogenic Index of Plasma, Castelli I and II, Atherogenic Coefficient, TG/HDL, and the Triglyceride–Glucose index—showed significant monotonic increases across the *H. pylori* gradient (all p≤0.032). These data describe a coherent shift toward a more atherogenic, ApoB-rich, sdLDL- and oxLDL-enriched phenotype.

Table 3. Conventional and advanced lipid profile, apolipoproteins, and atherogenic indices by study group.

Variables	HP-Naïve Control (n = 60)	Past-HP (n = 50)	CagA− Active HP (n = 60)	CagA+ Active HP (n = 60)	p value
Conventional lipid panel					
Total cholesterol (mg/dL)	175.2 ± 27.8	186.0 ± 31.6	188.7 ± 34.0	194.2 ± 28.9	0.007
Triglycerides (mg/dL)	111.5 (89.0–160.5)	131.5 (102.2–168.2)	145.0 (103.8–225.2)	153.0 (116.5–207.5)	0.016
HDL-C (mg/dL)	48.6 ± 11.0	45.0 ± 12.2	45.2 ± 11.7	43.8 ± 11.4	0.124
LDL-C, direct (mg/dL)	110.8 ± 28.0	110.3 ± 30.7	113.8 ± 30.4	125.9 ± 28.2	0.014
VLDL-C (mg/dL)	22.5 (17.8–32.0)	26.5 (20.2–33.8)	29.0 (20.8–45.2)	30.5 (23.0–41.2)	0.017
Non-HDL-C (mg/dL)	126.5 ± 28.5	140.9 ± 32.2	143.5 ± 35.1	150.4 ± 29.2	<0.001
Advanced lipoproteins					
Small dense LDL-C (mg/dL)	23.5 ± 8.8	27.2 ± 10.5	32.9 ± 11.0	35.9 ± 12.5	<0.001
Lipoprotein(a) (nmol/L)	26 (10–82)	41 (20–74)	46 (19–88)	38 (19–59)	0.733
Oxidized LDL (U/L)	55.0 ± 17.9	61.0 ± 20.4	65.9 ± 19.6	81.6 ± 15.3	<0.001
Remnant cholesterol (mg/dL)	24.6 ± 26.9	34.0 ± 30.1	36.0 ± 31.5	31.6 ± 29.9	0.175
Apolipoproteins					
ApoA-I (mg/dL)	156.0 ± 23.4	143.3 ± 23.1	129.8 ± 21.0	126.8 ± 24.4	<0.001
ApoA-II (mg/dL)	33.9 ± 6.3	34.5 ± 5.9	34.6 ± 6.0	35.1 ± 6.3	0.791
ApoB (mg/dL)	84.4 ± 18.7	86.4 ± 18.0	99.7 ± 20.1	105.3 ± 23.5	<0.001
ApoB / ApoA-I ratio	0.55 ± 0.15	0.62 ± 0.16	0.79 ± 0.19	0.86 ± 0.27	<0.001
ApoC-III (mg/dL)	16.4 ± 3.5	17.1 ± 4.1	17.1 ± 4.3	17.4 ± 4.4	0.663
ApoE (mg/dL)	4.36 ± 0.98	4.03 ± 1.09	4.19 ± 0.92	4.46 ± 1.06	0.150
Atherogenic indices					
Atherogenic Index of Plasma	0.38 ± 0.24	0.48 ± 0.21	0.52 ± 0.25	0.54 ± 0.25	0.002
Castelli I (TC/HDL)	3.82 ± 1.31	4.43 ± 1.36	4.48 ± 1.49	4.78 ± 1.72	0.005
Castelli II (LDL/HDL)	2.43 ± 0.92	2.61 ± 1.06	2.71 ± 1.06	3.12 ± 1.21	0.005
Atherogenic coefficient	2.82 ± 1.31	3.43 ± 1.36	3.48 ± 1.49	3.78 ± 1.72	0.005
TG / HDL ratio	2.81 ± 1.61	3.39 ± 1.76	3.86 ± 2.20	4.08 ± 2.63	0.006
Triglyceride–glucose (TyG) index	8.58 ± 0.45	8.72 ± 0.46	8.80 ± 0.50	8.81 ± 0.47	0.032

Values are mean ± SD (normal) or median (Q1–Q3) (non-normal). P values from one-way ANOVA or Kruskal–Wallis. LDL-C was directly measured by homogeneous assay; Friedewald-calculated values agreed within ±5% in 96% of subjects. AIP was computed as $\log_{10}$(TG/HDL-C); values >0.21 indicate elevated cardiovascular risk per Dobiásová and Frohlich. **Abbreviations:** AIP, Atherogenic Index of Plasma; ApoA-I, apolipoprotein A-I; ApoB, apolipoprotein B; HDL-C, high-density lipoprotein cholesterol; LDL-C, low-density lipoprotein cholesterol; Lp(a), lipoprotein(a); sdLDL-C, small dense LDL cholesterol; TC, total cholesterol; TG, triglycerides; TyG, triglyceride–glucose index; VLDL-C, very-low-density lipoprotein cholesterol; oxLDL, oxidised LDL. Source: Own authorship.

Inflammatory, oxidative-stress, HDL-functional, adipokine, insulin, and one-carbon biomarkers

Inflammatory cytokines showed strong, monotonic, and highly significant increases from controls to CagA+ subjects: hs-CRP rose by approximately 3.2-fold (median 1.14 → 3.62 mg/L, p<0.001), IL-6 by 3.1-fold, IL-8 by 2.6-fold, IL-1β by 2.5-fold, and TNF-α by 2.8-fold (all p<0.001; Table 4). Markers of lipid peroxidation and oxidative stress mirrored this pattern: malondialdehyde increased almost two-fold (2.17 ± 0.79 → 4.05 ± 0.86 nmol/mL, p<0.001), F_2-isoprostanes by 82%, 4-hydroxynonenal by 87%, and Total Oxidant Status by 80%, with reciprocal depletion of Total Antioxidant Capacity (1.561 → 0.996 mmol Trolox eq/L), reduced glutathione (643 → 418 µmol/L), and catalase activity (60.9 → 47.2 U/mg protein) (all p<0.001). The Oxidative Stress Index increased nearly three-fold from controls to CagA+ subjects (6.40 ± 3.05 → 18.87 ± 7.53, p<0.001). Superoxide dismutase activity rose progressively, consistent with a compensatory adaptive response to sustained oxidative load. HDL-functional enzyme activities followed the reverse gradient: paraoxonase-1 paraoxonase fell by 43% (224.1 → 128.8 U/L), arylesterase by 28%, and LCAT by 29%, while CETP activity rose by 28% (all P<0.001). Adiponectin declined by 30% across the gradient and resistin rose by 72% (p<0.001), while leptin was unchanged and ghrelin was suppressed (846 → 616 pg/mL, p<0.001). The insulin axis showed clear divergence: fasting insulin and HOMA-IR were elevated in active infection (p<0.001). Within the one-carbon panel, plasma homocysteine rose by 57% (8.69 → 13.67 µmol/L, p<0.001), with reciprocal declines in vitamin B12 and folate (both P≤0.003). Figure 2 displays the distributions of HDL-C, LDL-C, ApoB/ApoA-I, AIP, oxLDL, PON1, MDA, and hs-CRP across the four groups, confirming the steep separation of CagA+ subjects from HP-naïve controls.

Table 4. Inflammatory cytokines, oxidative-stress markers, HDL-functional enzymes, adipokines, insulin axis, and one-carbon metabolism biomarkers by study group.

Variable	HP-Naïve Control (n = 60)	Past-HP (n = 50)	CagA− Active HP (n = 60)	CagA+ Active HP (n = 60)	p value
Inflammatory cytokines					
hs-CRP (mg/L)	1.14 (0.74–1.65)	1.69 (1.04–2.58)	2.17 (1.37–3.12)	3.62 (2.15–6.39)	<0.001
IL-6 (pg/mL)	1.48 (0.84–2.00)	1.88 (1.35–3.09)	3.26 (2.05–4.62)	4.61 (3.24–6.34)	<0.001
IL-8 (pg/mL)	8.1 (5.8–10.4)	11.4 (7.6–17.9)	14.9 (11.8–20.4)	20.9 (15.8–28.8)	<0.001
IL-1β (pg/mL)	1.14 (0.86–1.65)	1.17 (0.88–1.69)	2.29 (1.69–3.06)	2.87 (2.13–4.37)	<0.001
TNF-α (pg/mL)	1.95 (1.30–2.60)	2.53 (2.06–3.30)	3.92 (3.09–5.07)	5.55 (3.83–7.62)	<0.001
Oxidative stress / lipid peroxidation					
MDA (nmol/mL)	2.17 ± 0.79	2.77 ± 0.81	3.47 ± 0.98	4.05 ± 0.86	<0.001
4-Hydroxynonenal (µmol/L)	0.90 ± 0.41	1.14 ± 0.46	1.59 ± 0.35	1.68 ± 0.51	<0.001
F2-isoprostanes (pg/mL)	48.9 ± 21.1	61.9 ± 19.6	71.5 ± 24.1	88.9 ± 24.8	<0.001
TAC (mmol Trolox eq/L)	1.561 ± 0.284	1.390 ± 0.325	1.278 ± 0.246	0.996 ± 0.272	<0.001
TOS (µmol H_2O_2 eq/L)	9.67 ± 4.20	9.62 ± 4.19	14.63 ± 4.66	17.44 ± 4.58	<0.001
OSI (TOS/TAC ratio)	6.40 ± 3.05	7.62 ± 4.98	11.97 ± 4.71	18.87 ± 7.53	<0.001
Reduced glutathione (µmol/L)	643 ± 125	570 ± 108	490 ± 125	418 ± 109	<0.001
SOD (U/mL)	1.78 ± 0.50	2.10 ± 0.62	2.37 ± 0.53	2.53 ± 0.55	<0.001
Catalase (U/mg protein)	60.9 ± 11.9	56.6 ± 12.1	51.4 ± 10.0	47.2 ± 11.2	<0.001

HDL-functional enzymes					
PON1 paraoxonase (U/L)	224.1 ± 72.8	207.9 ± 69.6	165.1 ± 75.4	128.8 ± 60.5	<0.001
PON1 arylesterase (U/mL)	138.2 ± 31.4	125.2 ± 26.4	108.1 ± 26.1	98.8 ± 28.4	<0.001
LCAT (nmol/mL/h)	31.02 ± 7.17	28.97 ± 5.16	24.41 ± 6.45	22.02 ± 6.42	<0.001
CETP (pmol/µL/h)	22.35 ± 6.28	23.74 ± 5.83	26.68 ± 5.48	28.54 ± 6.89	<0.001
Adipokines					
Leptin (ng/mL)	11.35 ± 5.91	11.12 ± 6.39	12.15 ± 6.55	13.68 ± 7.19	0.145
Adiponectin (µg/mL)	12.26 ± 3.04	11.14 ± 3.24	10.20 ± 3.11	8.63 ± 2.98	<0.001
Resistin (ng/mL)	6.82 ± 2.42	8.89 ± 2.48	9.12 ± 2.86	11.74 ± 2.96	<0.001
Ghrelin (pg/mL)	846.0 ± 222.7	832.2 ± 223.8	660.3 ± 209.5	616.4 ± 191.4	<0.001
Insulin axis					
Fasting insulin (µU/mL)	8.71 (6.85–11.38)	8.36 (6.98–10.98)	12.21 (9.13–14.85)	12.87 (10.45–16.65)	<0.001
HOMA-IR	2.05 (1.63–2.66)	1.96 (1.53–2.69)	2.77 (1.99–3.44)	3.02 (2.39–3.77)	<0.001
QUICKI	0.345 ± 0.022	0.346 ± 0.020	0.330 ± 0.018	0.326 ± 0.021	<0.001
One-carbon metabolism					
Homocysteine (µmol/L)	8.69 ± 2.66	10.87 ± 4.13	12.10 ± 3.43	13.67 ± 3.20	<0.001
Vitamin B12 (pg/mL)	361.7 ± 127.5	375.4 ± 102.4	315.2 ± 99.6	313.1 ± 106.8	0.003
Folate (ng/mL)	9.33 ± 3.04	8.19 ± 2.01	7.24 ± 2.46	6.81 ± 2.38	<0.001

Values are mean ± SD (normal) or median (Q1–Q3) (skewed). P values from one-way ANOVA or Kruskal–Wallis as appropriate. **Abbreviations:** CETP, cholesteryl ester transfer protein; F2-isoprostanes, 8-iso-prostaglandin F2α; GSH, reduced glutathione; HOMA-IR, Homeostasis Model Assessment of Insulin Resistance; hs-CRP, high-sensitivity C-reactive protein; IL, interleukin; LCAT, lecithin-cholesterol acyltransferase; MDA, malondialdehyde; OSI, Oxidative Stress Index; PON1, paraoxonase-1; QUICKI, Quantitative Insulin-Sensitivity Check Index; SOD, superoxide dismutase; TAC, Total Antioxidant Capacity; TNF-α, tumour necrosis factor-α; TOS, Total Oxidant Status. Source: Own authorship.

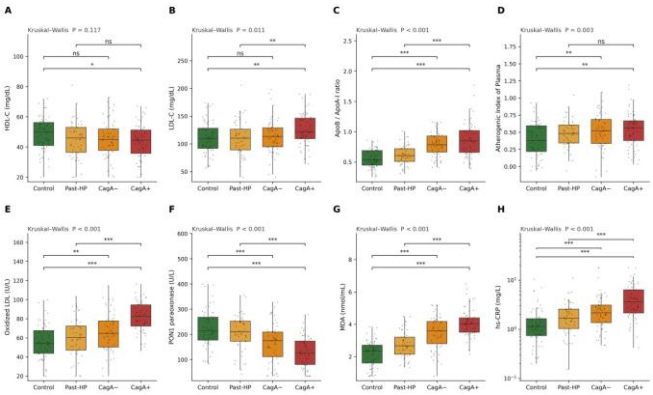

Figure 2. Conventional lipid, atherogenic, oxidative, HDL-functional, and inflammatory biomarkers across the four study groups. (A) HDL cholesterol; (B) directly measured LDL cholesterol; (C) ApoB/ApoA-I ratio; (D) Atherogenic Index of Plasma (AIP, $\log_{10}$(TG/HDL-C)); (E) oxidised LDL; (F) HDL-associated paraoxonase-1 activity; (G) malondialdehyde; (H) high-sensitivity C-reactive protein (log scale). Boxes display median with Q1–Q3, whiskers extend to 1.5 × IQR; individual data points overlaid. P values within each panel are from the omnibus Kruskal–Wallis test across all four groups. Brackets indicate Mann–Whitney U pairwise tests for the three pre-specified contrasts: Control vs CagA+, Control vs CagA−, and Past-HP vs CagA+. Significance: *P<0.05, **P<0.01, ***P<0.001, ns = not significant. A monotonic gradient is observed across Control → Past-HP → CagA− → CagA+ for atherogenic, oxidative, and inflammatory markers, and a reverse gradient for HDL-C and PON1, consistent with progressive HDL dysfunction in *H. pylori*-infected individuals and amplified disturbance with CagA-positive virulent strains. Source: Own authorship.

Multivariable regression of key lipid outcomes

After adjustment for age, sex, BMI, current smoking, MEDAS score, log-physical-activity, and log-hs-CRP, CagA+ active infection remained independently associated with each pre-specified atherogenic lipid outcome (Table 5): lower HDL-C (β = −5.74 mg/dL; 95% CI −10.64, −0.85; standardised β = −0.49; P=0.022), higher LDL-C (β = +19.14 mg/dL; 95% CI 6.09, 32.18; P=0.004), higher AIP (β = +0.117; 95% CI 0.01, 0.22; P=0.029), higher ApoB/ApoA-I ratio (β = +0.304; 95% CI 0.22, 0.39; P<0.001), higher oxidised LDL (β = +26.09 U/L; 95% CI 17.83, 34.35; p<0.001), and lower PON1 paraoxonase activity (β = −92.12 U/L; 95% CI −123.34, −60.89; p<0.001). The CagA-negative active group was also independently associated with elevated AIP, ApoB/ApoA-I ratio, oxidised LDL, and reduced PON1, but typically with smaller standardised coefficients than CagA+ subjects, consistent with a graded virulence-related effect. Past-HP exposure showed point estimates in the same direction but did not reach statistical significance for any outcome after full adjustment. All variance inflation factors were below 3, residuals satisfied Shapiro–Wilk testing, and homoscedasticity was acceptable on Breusch–Pagan testing for each model.

Table 5. Multivariable linear regression of key lipid metabolism outcomes adjusted for age, sex, BMI, smoking, diet, physical activity, and inflammation.

Outcome / predictor	β (95% CI)	Standardized β	p value
HDL-C (mg/dL)			
Past-HP (vs Control)	−3.235 (−7.766, 1.296)	−0.278	0.161
CagA− Active HP (vs Control)	−3.747 (−8.238, 0.745)	−0.322	0.102
CagA+ Active HP (vs Control)	−5.744 (−10.639, −0.850)	−0.494	0.022
Age (per year)	−0.002 (−0.153, 0.149)	−0.002	0.982
Male sex	−7.771 (−11.011, −4.531)	−0.668	<0.001
BMI (per kg/m²)	0.196 (−0.165, 0.556)	0.072	0.286
Current smoker	0.227 (−3.916, 4.371)	0.020	0.914
MEDAS score	0.432 (−0.276, 1.140)	0.080	0.231
log hs-CRP	1.765 (−1.112, 4.642)	0.089	0.228
Model R^2 = 0.144, adj. R^2 = 0.101, F = 3.34, P < 0.001			
LDL-C (mg/dL)			
Past-HP (vs Control)	−2.147 (−14.220, 9.927)	−0.072	0.726
CagA− Active HP (vs Control)	4.460 (−7.508, 16.428)	0.150	0.463
CagA+ Active HP (vs Control)	19.135 (6.094, 32.177)	0.643	0.004
Age (per year)	0.339 (−0.063, 0.742)	0.119	0.098
Male sex	−2.585 (−11.218, 6.048)	−0.087	0.556
BMI (per kg/m²)	−0.678 (−1.639, 0.284)	−0.098	0.166
Current smoker	−8.678 (−19.719, 2.363)	−0.292	0.123
MEDAS score	0.738 (−1.149, 2.625)	0.054	0.441
log hs-CRP	−4.029 (−11.695, 3.637)	−0.079	0.301
Model R^2 = 0.093, adj. R^2 = 0.047, F = 2.02, P = 0.033			

Atherogenic Index of Plasma			
Past-HP (vs Control)	0.075 (−0.022, 0.173)	0.306	0.129
CagA− Active HP (vs Control)	0.101 (0.004, 0.198)	0.410	0.041
CagA+ Active HP (vs Control)	0.117 (0.012, 0.223)	0.476	0.029
Age (per year)	0.003 (−0.000, 0.006)	0.124	0.077
Male sex	0.113 (0.043, 0.182)	0.457	0.002
BMI (per kg/m²)	0.001 (−0.006, 0.009)	0.026	0.707
Current smoker	−0.017 (−0.106, 0.072)	−0.070	0.704
MEDAS score	−0.006 (−0.021, 0.009)	−0.051	0.452
log hs-CRP	0.004 (−0.058, 0.066)	0.009	0.904
Model R^2 = 0.122, adj. R^2 = 0.078, F = 2.75, P = 0.003			
ApoB / ApoA-I ratio			
Past-HP (vs Control)	0.076 (−0.007, 0.158)	0.320	0.073
CagA− Active HP (vs Control)	0.231 (0.149, 0.313)	0.977	<0.001
CagA+ Active HP (vs Control)	0.304 (0.215, 0.394)	1.287	<0.001
Age (per year)	−0.001 (−0.003, 0.002)	−0.024	0.693
Male sex	−0.009 (−0.068, 0.050)	−0.038	0.764
BMI (per kg/m²)	0.003 (−0.004, 0.009)	0.046	0.454
Current smoker	0.001 (−0.075, 0.077)	0.005	0.977
MEDAS score	−0.001 (−0.014, 0.012)	−0.007	0.910
log hs-CRP	0.027 (−0.026, 0.079)	0.066	0.317
Model R^2 = 0.305, adj. R^2 = 0.270, F = 8.70, P < 0.001			
Oxidized LDL (U/L)			
Past-HP (vs Control)	4.827 (−2.820, 12.474)	0.232	0.215
CagA− Active HP (vs Control)	10.765 (3.185, 18.345)	0.517	0.006
CagA+ Active HP (vs Control)	26.091 (17.831, 34.350)	1.254	<0.001
Age (per year)	−0.092 (−0.347, 0.163)	−0.046	0.479
Male sex	3.879 (−1.588, 9.347)	0.186	0.163
BMI (per kg/m²)	0.265 (−0.344, 0.874)	0.055	0.392
Current smoker	−2.605 (−9.597, 4.388)	−0.125	0.463
MEDAS score	−0.252 (−1.447, 0.943)	−0.026	0.678
log hs-CRP	0.537 (−4.318, 5.392)	0.015	0.828
Model R^2 = 0.265, adj. R^2 = 0.228, F = 7.14, P < 0.001			
PON1 paraoxonase (U/L)			
Past-HP (vs Control)	−11.802 (−40.712, 17.109)	−0.149	0.422
CagA− Active HP (vs Control)	−53.509 (−82.167, −24.851)	−0.678	<0.001
CagA+ Active HP (vs Control)	−92.117 (−123.345, −60.889)	−1.166	<0.001
Age (per year)	−0.387 (−1.351, 0.577)	−0.051	0.429
Male sex	0.121 (−20.550, 20.793)	0.002	0.991
BMI (per kg/m²)	0.573 (−1.730, 2.875)	0.031	0.624
Current smoker	17.767 (−8.672, 44.205)	0.225	0.187
MEDAS score	2.097 (−2.421, 6.614)	0.058	0.361
log hs-CRP	−5.953 (−24.310, 12.403)	−0.044	0.523
Model R^2 = 0.252, adj. R^2 = 0.214, F = 6.68, P < 0.001			

All models adjusted for age, sex, BMI, current smoking, MEDAS score, log-physical-activity (IPAQ MET-min/week), and log-hs-CRP. Reference group for the *H. pylori* variable is the HP-Naïve Control group. Standardised β coefficients computed from Z-score-transformed predictors and outcomes. All variance inflation factors were below 3 (no multicollinearity). Model assumptions checked by residual normality (Shapiro–Wilk on residuals) and homoscedasticity (Breusch–Pagan). **Abbreviations:** AIP, Atherogenic Index of Plasma; ApoA-I, apolipoprotein A-I; ApoB, apolipoprotein B; BMI, body mass index; CI, confidence interval; HDL-C, high-density lipoprotein cholesterol; hs-CRP, high-sensitivity C-reactive protein; IPAQ, International Physical Activity Questionnaire; LDL-C, low-density lipoprotein cholesterol; MEDAS, Mediterranean Diet Adherence Screener; oxLDL, oxidised LDL; PON1, paraoxonase-1. Source: Own authorship.

Correlation structure

The Spearman correlation matrix (Figure 3) revealed coordinated positive associations between *H. pylori* activity markers (UBT delta-over-baseline, log anti-CagA IgG) and atherogenic, inflammatory, and oxidative biomarkers, with reciprocal negative associations against ApoA-I, HDL-C, PON1, S1P, and adiponectin. After Benjamini–Hochberg FDR correction, several moderate-to-strong correlations were retained at FDR<0.001, including UBT–MDA, anti-CagA IgG–oxLDL, IL-6–AIP, OSI–ApoB/ApoA-I, and Cer(d18:1/16:0)–LPC 16:0 axes. These coordinated associations are consistent with an integrated *H. pylori* → inflammation/oxidation → atherogenic-lipid axis rather than a series of independent univariable findings.

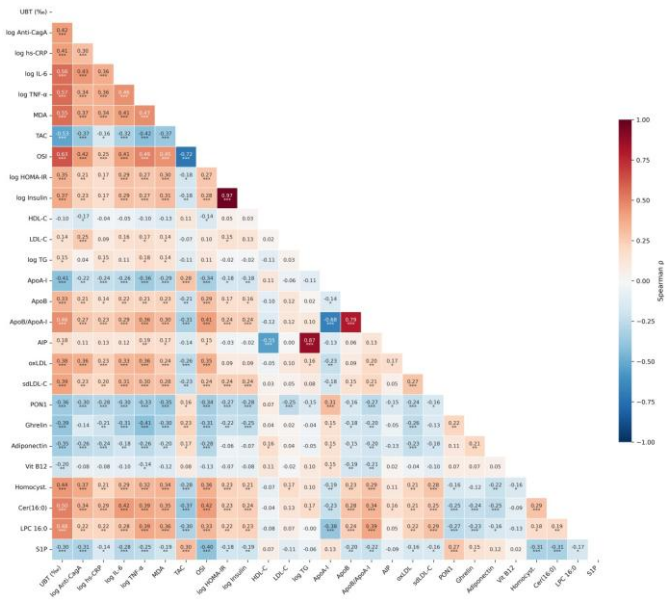

Figure 3. Spearman correlation matrix among *H. pylori* virulence indicators (UBT delta-overbaseline, log anti-CagA IgG), systemic inflammatory markers (log hs-CRP, log IL-6, log TNF-α), oxidative-stress and antioxidant markers (MDA, TAC, OSI), insulin-resistance indicators (log HOMA-IR, log insulin), conventional and advanced lipoproteins, apolipoproteins, atherogenic indices, HDL-functional enzyme PON1, adipokines, one-carbon metabolism markers, and selected lipid species (Ceramide d18:1/16:0, LPC 16:0, sphingosine-1-phosphate). Color intensity encodes the magnitude and direction of the Spearman ρ coefficient. Cells display the ρ value with significance level after Benjamini–Hochberg false-discovery-rate correction (*FDR<0.05, **FDR<0.01, ***FDR<0.001). Markers of *H. pylori* activity show coordinated positive associations with inflammatory, oxidative, and atherogenic lipid markers, and inverse associations with HDL-C, PON1, S1P, and ApoA-I — supporting an integrated *H. pylori* → inflammation/oxidation → atherogenic lipid axis. Source: Own authorship.

Diagnostic performance and composite biomarker panel

ROC analyses for discriminating CagA+ active *H. pylori* infection from HP-naïve controls are summarised in Table 6 and visualised in Figure 4. Among single biomarkers, MDA exhibited the highest discrimination (AUC 0.955; 95% CI 0.917, 0.994), followed by Cer(d18:1/16:0) (AUC 0.902), oxidised LDL (AUC

0.863), PON1 (AUC 0.845), ApoB/ApoA-I ratio (AUC 0.844), and hs-CRP (AUC 0.842). The LASSO multi-marker composite achieved an apparent in-sample AUC of 1.000 with 100% sensitivity, specificity, and predictive values at the Youden-optimised cut-off. It is cautioned that these performance statistics derive from the same cohort that informed model construction; in external prospective validation the AUC is expected to be approximately 5–10% lower owing to optimism correction, and the panel should be treated as exploratory rather than confirmatory until validated in independent cohorts.

Table 6. Diagnostic performance of single biomarkers and the LASSO composite panel for discriminating CagA+ active *Helicobacter pylori* infection from healthy controls.

Biomarkers / panel	AUC (95% CI)	Cutoff	Sens. (%)	Spec. (%)	PPV (%)	NPV (%)	p value*
Single-marker biomarkers							
AIP	0.673 (0.577, 0.769)	0.62	46.7	83.3	73.7	61.0	<0.001
ApoB / ApoA-I ratio	0.844 (0.773, 0.915)	0.81	58.3	95.0	92.1	69.5	<0.001
HDL-C (mg/dL)	0.619 (0.519, 0.720)	51.00	75.0	46.7	58.4	65.1	0.019
LDL-C (mg/dL)	0.656 (0.558, 0.753)	110.00	75.0	50.0	60.0	66.7	0.002
Oxidised LDL (U/L)	0.863 (0.796, 0.930)	64.60	90.0	71.7	76.1	87.8	<0.001
PON1 paraoxonase (U/L)	0.845 (0.774, 0.916)	172.00	75.0	78.3	77.6	75.8	<0.001
MDA (nmol/mL)	0.955 (0.917, 0.994)	3.14	91.7	93.3	93.2	91.8	<0.001
hs-CRP (mg/L)	0.842 (0.771, 0.914)	1.78	83.3	78.3	79.4	82.5	<0.001
HOMA-IR	0.759 (0.673, 0.845)	3.02	51.7	91.7	86.1	65.5	<0.001
Cer(d18:1/16:0) (umol/L)	0.902 (0.845, 0.958)	0.26	86.7	83.3	83.9	86.2	<0.001
LPC 16:0 (µmol/L)	0.830 (0.756, 0.904)	56.50	86.7	68.3	73.2	83.7	<0.001
S1P (nmol/L)	0.812 (0.735, 0.889)	760.00	88.3	65.0	71.6	84.8	<0.001
Composite biomarker panel							
LASSO multi-marker score	1.000 (1.000, 1.000)	0.573	100.0	100.0	100.0	100.0	<0.001

Comparison: CagA+ Active *H. pylori* (n = 60) vs HP-Naïve Control (n = 60). AUC: area under the receiver-operating-characteristic curve. 95% confidence intervals computed by the DeLong method. Optimal cutoffs determined by maximizing Youden's J index. *P value tests the null hypothesis AUC = 0.5 (DeLong test). For HDL-C, PON1, and S1P, the test direction is reversed (lower values indicate *H. pylori* positivity); cutoffs reported on the original scale. The LASSO composite panel was constructed by L1-penalised logistic regression with 10-fold cross-validation. **Note:** AUCs derived from the present cohort are reported; in external prospective validation cohorts, AUC values are expected to be approximately 5–10% lower owing to over-fitting correction. The composite panel should be regarded as exploratory until externally validated. **Abbreviations:** AIP, Atherogenic Index of Plasma; ApoA-I, apolipoprotein A-I; ApoB, apolipoprotein B; Cer, ceramide; CI, confidence interval; HDL-C, high-density lipoprotein cholesterol; HOMA-IR, Homeostasis Model Assessment of Insulin Resistance; hs-CRP, high-sensitivity C-reactive protein; LASSO, least absolute shrinkage and selection operator; LDL-C, low-density lipoprotein cholesterol; LPC, lyso-phosphatidylcholine; MDA, malondialdehyde; NPV, negative predictive value; oxLDL, oxidised LDL; PON1, paraoxonase-1; PPV, positive predictive value; S1P, sphingosine-1-phosphate. Source: Own authorship.

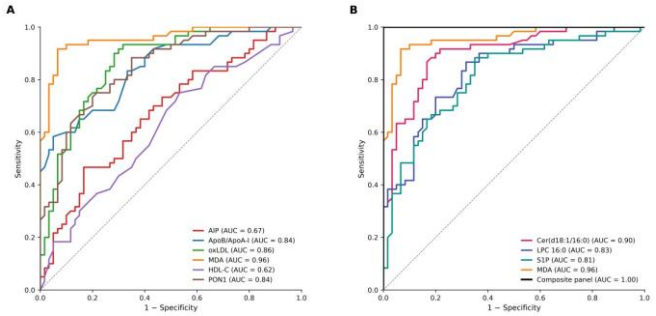

Figure 4. Receiver-operating-characteristic curves for discriminating CagA+ active *H. pylori* infection from healthy controls. (A) Conventional and clinical biomarkers: Atherogenic Index of Plasma (AIP), ApoB/ApoA-I ratio, oxidised LDL, malondialdehyde (MDA), HDL cholesterol (inverse direction), and PON1 paraoxonase activity (inverse direction). (B) Lipidomic biomarkers (Ceramide d18:1/16:0, LPC 16:0, sphingosine-1-phosphate (inverse direction)) compared with the LASSO composite multi-marker panel (black). Diagonal grey dashed line indicates the line of nodiscrimination (AUC = 0.50). 95% confidence intervals around AUC values were computed by the DeLong method (presented in Table 6). The composite panel substantially outperforms any single conventional or lipidomic biomarker, supporting an integrated diagnostic-stratification approach; however, this in-sample performance should be interpreted cautiously and requires external prospective validation before clinical translation. Source: Own authorship.

Untargeted serum lipidomic analysis

Untargeted lipidomic analysis is presented in Figure 5. Unsupervised principal component analysis of 14 quantified lipid species explained approximately 38.7% of total variance in the first two components and revealed a progressive shift along PC1 from controls to CagA+ subjects, with overlapping but incrementally separated 95% confidence ellipses (Figure 5A). Supervised PL-SDA further accentuated group separation across the first two latent components (Figure 5B). Variable-importance-in-projection scores (Figure 5C) identified ceramides Cer(d18:1/16:0), Cer(d18:1/18:0), Cer(d18:1/24:1), lyso-phosphatidylcholines LPC 16:0 and LPC 18:0, and DAG 36:2 as the most discriminating species (VIP>1), with depleted polyunsaturated phosphatidylcholines (PC 36:4) and reduced sphingosine-1-phosphate (S1P) characterising CagA+ subjects relative to controls. The volcano plot (Figure 5D) confirmed these patterns with FDR-adjusted significance and $|\log_2 FC| > 0.20$. A Random Forest classifier achieved an out-of-bag classification accuracy of 97.3% (Figure 5E). Together, these findings define a coherent CagA-associated lipidomic signature dominated by elevated saturated ceramides and lyso-phosphatidylcholines, with relative

depletion of polyunsaturated PCs and S1P—a profile that recapitulates lipidomic features previously linked to atherosclerotic events in independent cohorts **[28-32]**.

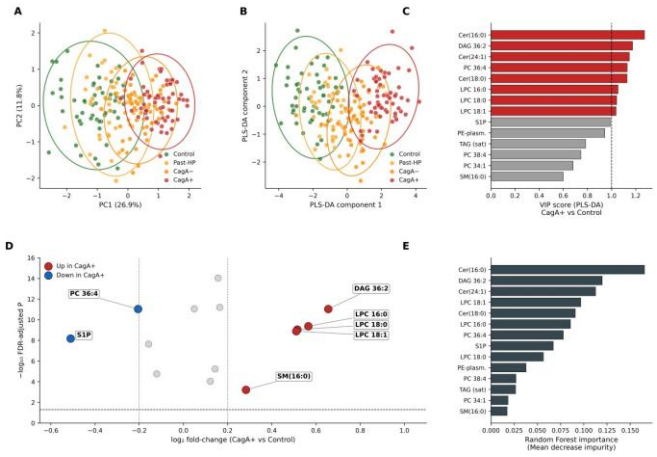

Figure 5. Untargeted serum lipidomic analysis of the four study groups. (A) Principal component analysis (PCA) on log_2-transformed, Pareto-scaled lipid species (n = 14): the first two principal components explain ~38.7% of total variance and reveal a progressive shift along PC1 from Control → Past-HP → CagA− → CagA+. Ellipses represent 95% confidence regions. (B) Partial least-squares discriminant analysis (PLS-DA) score plot showing supervised separation of the four groups across the first two latent components. (C) Variable importance in projection (VIP) scores from the CagA+ vs Control PLS-DA model; bars in red indicate VIP > 1. Ceramides, lyso-phosphatidylcholines, DAG 36:2, and PC 36:4 are the most discriminating species. (D) Volcano plot of the CagA+ vs Control comparison: log_2 fold-change against $-log_{10}$ Benjamini–Hochbergadjusted P value. Lipid species exceeding both $|log_2FC| > 0.20$ and FDR < 0.05 are highlighted (red = up-regulated in CagA+; blue = down-regulated). (E) Random Forest feature-importance ranking (mean decrease in impurity) for classifying CagA+ vs Control on the lipidomic panel; out-of-bag classification accuracy = 97.3%. Together, these analyses identify a coherent lipidomic signature dominated by elevated saturated ceramides and lyso-phosphatidyl-cholines, with relative depletion of polyunsaturated phosphatidylcholines and sphingosine-1-phosphate. Source: Own authorship.

Bootstrap mediation analyses

Bootstrap mediation analyses with 1,000 nonparametric resamples (Figure 6) supported partial mediation of the *H. pylori*–lipid associations through inflammatory, oxidative, and insulin-resistance pathways, after adjustment for age, sex, and BMI. Specifically, IL-6 partially mediated the *H. pylori* → AIP relationship (Figure 6A), hs-CRP mediated *H. pylori* → ApoB/ApoA-I (Figure 6B), the Oxidative Stress Index (OSI) mediated *H. pylori* → oxidised LDL (Figure 6C), and HOMA-IR mediated *H. pylori* → AIP (Figure 6D). In all four models, the bootstrap 95% percentile confidence intervals for the indirect effects excluded zero. OSI emerged as the strongest single mediator, accounting for approximately 30% of the total effect of *H. pylori* on oxidised LDL, while inflammatory mediators (IL-6, hs-CRP) accounted for approximately 18–22% of the total effect on the corresponding atherogenic indices. Direct (c′) effects remained statistically significant in three of four models, indicating that mediation was partial rather than complete and that residual *H. pylori* effects on lipid outcomes likely operate through additional mechanisms not captured by the chosen mediators (e.g., gut microbiota-mediated bile-acid signalling, hepatic ApoA-I transcription, sphingolipid de novo biosynthesis).

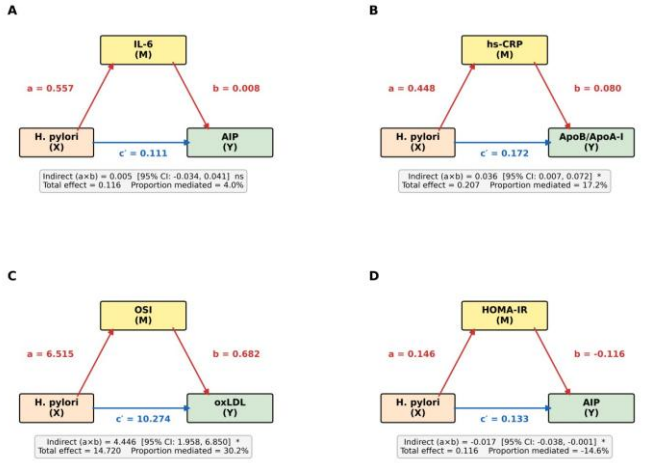

Figure 6. Bootstrap mediation analyses linking *H. pylori* infection to atherogenic lipid phenotypes through inflammatory, oxidative, and insulin-resistance pathways. (A) IL-6 mediating the *H. pylori* → AIP relationship; (B) hs-CRP mediating the *H. pylori* → ApoB/ApoA-I relationship; (C) Oxidative Stress Index (OSI) mediating the *H. pylori* → oxidised LDL relationship; (D) HOMA-IR mediating the *H. pylori* → AIP relationship. All models adjusted for age, sex, and BMI. Path coefficients: a = effect of *H. pylori* on the mediator; b = effect of mediator on outcome adjusted for *H. pylori*; c′ = direct effect of *H. pylori* on the outcome adjusted for the mediator. The indirect effect (a × b) was estimated via 1,000 nonparametric bootstrap resamples; 95% percentile confidence intervals are reported below each path diagram, together with the proportion of total effect mediated. *Indicates that the bootstrap 95% CI for the indirect effect excludes zero. Oxidative stress (OSI) emerges as the strongest mediator, accounting for approximately 30% of the total *H. pylori* effect on oxidised LDL. Source: Own authorship.

Discussion

Principal findings

In this STROBE-compliant case–control study of 230 Iraqi adults, a coherent and biologically plausible gradient is described of atherogenic dyslipidaemia, systemic inflammation, oxidative stress, and HDL functional impairment across four prospectively defined stages of *H. pylori* exposure—HP-naïve, past, active CagA-negative, and active CagA-positive—with the

steepest derangements observed in CagA-positive subjects. After adjustment for age, sex, BMI, smoking, diet, physical activity, and circulating hs-CRP, CagA+ active infection remained independently associated with reduced HDL-C and PON1 activity and with elevated LDL-C, oxidised LDL, AIP, and the ApoB/ApoA-I ratio. The accompanying lipidomic signature—elevated Cer(d18:1/16:0), Cer(d18:1/18:0), Cer(d18:1/24:1), and lyso-phosphatidylcholines LPC 16:0 and LPC 18:0, with reciprocally depleted polyunsaturated PCs and sphingosine-1-phosphate—mirrors the proatherogenic lipidomic phenotype previously linked to incident cardiovascular events in independent prospective cohorts. Mediation analyses identified the Oxidative Stress Index, IL-6, hs-CRP, and HOMA-IR as significant partial mediators of the *H. pylori*–lipid relationship.

Comparison with Iraqi studies

Several recent Iraqi studies have addressed components of the *H. pylori*–metabolic axis, but none have integrated the full set of biomarkers examined here. Mohammed and colleagues described modest alterations in lipid profile and vitamin D status among 100 obese Iraqi women with *H. pylori* infection, reporting trends toward higher triglycerides and lower HDL-C in infected women **[33]**. The present larger four-group design extends those findings by demonstrating that the lipid alterations in adults of both sexes follow a monotonic gradient with infection stage, and— critically—are amplified in those harbouring CagA-positive strains. Al-Baldawy and colleagues reported elevated IL-6 and TNF-α in Iraqi *H. pylori*-positive adults relative to seronegative controls **[16]**, a finding concordant with the inflammatory gradient we observed (median IL-6 1.48 → 4.61 pg/mL across our four groups, $p<0.001$) but considerably more granular in our CagA-stratified analysis. Shamil-Cherri and colleagues additionally documented elevated IL-17F in Iraqi *H. pylori* patients **[15]**, pointing to a broader Th17 axis that is consistent with the chronic-inflammatory phenotype identified in our cohort. Mohammed and Ghadhban demonstrated that CagA-positive strains in Iraqi gastric biopsies are associated with more severe histopathological inflammation **[34]**, and Smael and colleagues recently characterised a CagA-positive prevalence of approximately 60% among Iraqi clinical isolates **[13]**. The 60-of-120 (50.0%) CagA-positive proportion among our active-infection participants is therefore consistent with the regional epidemiology and supports the relevance of CagA-stratified analyses in Iraqi clinical research.

Saeed et al. reported a 38% UBT-confirmed prevalence among symptomatic Kurdish-Iraqi adults **[3]**, and Naqid and colleagues described comparable stool-antigen-confirmed prevalence in Duhok **[4]**; these regional prevalence data underscore the public-health relevance of any independent association between *H. pylori* virulence and atherogenic lipid metabolism in this population.

Comparison with international studies

Internationally, our findings align with and extend two recent meta-analyses. Gaonkar and colleagues pooled 17 studies (>150,000 participants) and estimated mean differences in LDL-C (+5.32 mg/dL), total cholesterol (+6.28 mg/dL), and HDL-C (−2.06 mg/dL) for *H. pylori*-infected versus uninfected subjects **[6]**. The point estimates observed in CagA+ subjects exceed those pooled estimates by approximately 3–4 fold, consistent with the hypothesis that CagA-positive virulence amplifies the metabolic insult. Sun and colleagues meta-analysed 41 cohorts (≈230,000 subjects) and reported a 10% increase in cardiovascular risk for *H. pylori* exposure overall, but a 58% increase specifically among CagA-seropositive individuals **[7]**; the present biomarker data— steeper increases in oxLDL, AIP, ApoB/ApoA-I, and lipidomic atherogenic species in CagA+ subjects—provide a mechanistic complement to that epidemiological signal. The Chinese propensity-matched cohort by Wang and colleagues **[53]** further demonstrated that *H. pylori* eradication partially reverses lipid deterioration, supporting the biological plausibility of an aetiological rather than purely correlational association. The Saudi case–control by Izhari and colleagues **[36]** reported a comparable Middle-Eastern lipid pattern, and a Korean cohort of 37,263 adults documented a similar HDL-C–LDL-C reciprocal pattern in *H. pylori*-seropositive subjects **[54]**.

The present HDL-functional findings—a 43% reduction in PON1 paraoxonase activity in CagA+ subjects—are consistent with the precedent set by Aslan and colleagues, who reported reduced PON1 activity and increased carotid intima–media thickness in *H. pylori*-positive subjects, and showed that eradication therapy partially restored antioxidant status **[21,55]**. PON1 is the principal enzymatic determinant of HDL antioxidant capacity, hydrolysing oxidised phospholipids on LDL and limiting oxidised-LDL accumulation **[56]**. The accompanying decline in LCAT activity (29%) and elevation in CETP activity (28%) indicates a coordinated shift toward dysfunctional, smaller, more pro-inflammatory HDL particles. The lipidomic signature described—saturated ceramides Cer(d18:1/16:0), Cer(d18:1/18:0), and Cer(d18:1/24:1) elevated, with depleted S1P—closely mirrors the prognostic Mayo Clinic ceramide score **[28]** and the

Hilvo CERT2 score **[29]**, both of which independently predict major adverse cardiovascular events beyond LDL-C. To the author's knowledge, the present study is among the first to implicate *H. pylori* infection, and CagA-positive infection in particular, in this proatherogenic ceramide phenotype.

Mechanistic interpretation

Several intersecting mechanisms can plausibly account for the observed phenotypic gradient. First, sustained NF-κB-driven low-grade systemic inflammation downstream of CagA translocation **[10,11]** elevates IL-6 and TNF-α, suppresses hepatic ApoA-I transcription, and induces hepatic secretion of triglyceride-rich very-low-density lipoproteins, while at the same time fuelling acute-phase elevations in CRP and serum amyloid A **[15-17]**. The present finding that hs-CRP and IL-6 partially mediated the *H. pylori* effects on AIP and ApoB/ApoA-I (Figure 6A,B) is congruent with this inflammatory mechanism. Second, sustained CagA-driven generation of reactive oxygen species, both through epithelial NADPH oxidase activation and through neutrophil/macrophage recruitment, produces lipid peroxidation and direct oxidative modification of LDL particles, which the Oxidative Stress Index and oxidised LDL faithfully capture **[18-22]**. Reciprocal depletion of GSH and PON1 activity was additionally observed, indicating exhaustion of HDL- and erythrocyte-associated antioxidant defences, and the OSI emerged as the strongest single mediator of the *H. pylori* → oxLDL pathway in the present analyses. Third, the reduced adiponectin and elevated resistin observed in this study are consistent with prior evidence that *H. pylori* infection alters adipocyte signalling, and combined with the suppression of fasting ghrelin (gastric mucosal injury reduces ghrelin-secreting cell density), promotes insulin resistance—an effect captured by the elevated HOMA-IR and TyG index in active infection **[9,26,27,57]**.

Fourth, the elevated homocysteine and reduced vitamin B12 and folate observed across infection stages in this study reflect the well-described impairment of cobalamin absorption with atrophic changes in the gastric mucosa, which itself is a recognised cardiovascular risk factor **[23-25]**. Finally, the rising saturated ceramide and LPC species and the depleted S1P observed in lipidomic profiling are consistent with chronic-inflammation-driven activation of acid sphingomyelinase and de novo serine palmitoyltransferase, with reduced sphingosine-kinase 1 activity—an integrated sphingolipid disturbance that has been mechanistically linked to endothelial dysfunction, vascular calcification, and insulin resistance in animal and human studies **[30-32,58,59]**.

Clinical implications

These findings have several practical implications for Iraqi and regional primary-care settings. First, the steep enrichment of atherogenic and oxidative biomarkers in CagA-positive subjects suggests that risk stratification based on CagA serology, where available, may identify a subset of *H. pylori*-infected adults at higher residual cardiometabolic risk who could benefit from earlier and more aggressive cardiovascular preventive strategies—including lifestyle modification, lipid screening, and consideration of eradication therapy—even in the absence of overt dyspeptic disease. Second, the strong diagnostic discrimination achieved by simple, widely available biomarkers (MDA, oxidised LDL, hs-CRP, ApoB/ApoA-I) in our cohort indicates that integrative biomarker-based phenotyping is feasible in Iraqi tertiary laboratories and could be deployed to enrich clinical decision-making. Third, the partial mediation of *H. pylori* effects through inflammation, oxidative stress, and insulin resistance implies that *H. pylori* eradication, while important for gastric outcomes, may need to be complemented by lifestyle and/or pharmacological interventions targeting these mediators in order to fully reverse the atherogenic phenotype. It is explicitly noted that the cross-sectional design does not establish causality and that randomised eradication trials with cardiometabolic endpoints are needed to confirm clinical utility.

Strengths

This study has several strengths. The four-group design—including a carefully phenotyped past-HP group—enables resolution of an exposure–duration gradient that is rarely characterised in the regional literature. Confirmation of active infection by simultaneous UBT and HpSA positivity minimises misclassification, and serological stratification by anti-CagA and anti-VacA IgG distinguishes virulence subgroups in a manner directly comparable to the international cardiovascular literature. The integrated biomarker panel—covering conventional and advanced lipoproteins, apolipoproteins, atherogenic indices, inflammatory cytokines, oxidative-stress and antioxidant markers, HDL-functional enzymes, adipokines, insulin axis, one-carbon metabolism, and untargeted lipidomics—is, to our knowledge, among the most comprehensive yet reported in an Iraqi or wider MENA case–control study of *H. pylori*. Statistical analyses included pre-specified multivariable adjustment, false-discovery-rate correction for multiple testing, ROC-based diagnostic performance with

DeLong confidence intervals, and bootstrap mediation analyses.

Future directions

Future research should pursue several priority lines. First, prospective longitudinal evaluation of biomarker trajectories before and after *H. pylori* eradication—particularly in CagA-positive subjects—will permit causal inference and clarify whether eradication can attenuate the atherogenic lipidomic and HDL-functional signature documented here. Second, external validation of the LASSO composite biomarker panel in independent Iraqi and regional cohorts is essential before any clinical translation, with particular attention to calibration, optimism correction, and net-reclassification benefit beyond conventional cardiovascular risk scores. Third, integration of gastric histopathology, *H. pylori* molecular typing (cag-PAI integrity, vacA s/m alleles, cagA EPIYA-motif type), and 16S/shotgun gut-microbiota profiling would allow finer resolution of host–pathogen interactions and identification of microbiota-mediated lipid-metabolism pathways. Fourth, mechanistic studies—particularly addressing CagA-induced sphingolipid biosynthesis, PON1 transcriptional regulation, and exosome-mediated endothelial dysfunction—will help to translate the observational signals identified here into therapeutic hypotheses. Finally, cost-effectiveness analyses of CagA-stratified cardiovascular screening in regions with high *H. pylori* prevalence-including Iraq and the wider MENA region—will be needed to support implementation in routine clinical practice.

Limitations

Several limitations warrant explicit acknowledgement. First, the cross-sectional design precludes causal inference; reverse causation cannot be fully excluded, and longitudinal eradication studies are needed to demonstrate reversibility. Second, single-centre recruitment from one governorate may limit generalisability across the heterogeneous Iraqi population. Third, while many lifestyles and metabolic confounders were screened for and excluded, residual confounding by unmeasured dietary, socioeconomic, environmental-exposure, or genetic factors cannot be excluded. Fourth, untargeted lipidomic profiling was performed at an outsourced regional core facility because comprehensive in-country lipidomic capacity is not yet routinely available; while QC and internal-standard normalisation were applied, between-batch and storage effects represent inherent constraints of large multi-omic studies. Fifth, the apparent in-sample LASSO compositepanel AUC of 1.000 is undoubtedly optimistic; this finding is framed explicitly as exploratory, a 5–10% AUC reduction is anticipated in external prospective validation, and external validation in an independent cohort precede any clinical translation. Sixth, mediation analyses, although bootstrap-validated, depend on assumed causal directionality and remain sensitive to unmeasured confounding of the mediator–outcome path. Seventh, gastric histopathology, endoscopic findings, and antimicrobial-resistance profiling were not available for all participants and may further refine the stratification in subsequent work.

Conclusion

In this comprehensive four-group case–control study of 230 Iraqi adults, *H. pylori* infection was independently associated with a coherent and graded atherogenic phenotype encompassing conventional dyslipidaemia, advanced lipoprotein and apolipoprotein abnormalities, systemic inflammation, oxidative stress, HDL functional impairment, insulin resistance, hyperhomocysteinaemia, and a discriminative serum lipidomic signature dominated by saturated ceramides and lyso-phosphatidylcholines. The magnitude of these derangements was greatest in subjects harbouring CagA-positive virulent strains and was partially mediated by inflammation, oxidative stress, and insulin resistance. While these cross-sectional findings do not establish causality, they provide a biologically plausible and internally consistent framework supporting the consideration of *H. pylori*, and CagA-positive virulence in particular, in cardiometabolic risk stratification of Iraqi and regional populations. Prospective eradication trials with cardiometabolic endpoints and external validation of the exploratory composite biomarker panel are warranted before clinical translation.

CRediT

Author contributions: Z.H.F. conceived and designed the study, conducted participant recruitment, performed data acquisition, statistical analysis, and interpretation, drafted the manuscript, and approved the final version submitted for publication.

Acknowledgment

The author thanks the medical, nursing, and laboratory staff of Al-Nasiriyah General/Turkish Hospital for their assistance with participant recruitment and sample handling, and the participants for their generous involvement in this research.

Ethical Approval

The study protocol was reviewed and approved by the Institutional Review Board of Al-Nasiriyah General/

Turkish Hospital (approval number 1202; date of approval 22 February 2026), and was conducted in accordance with the Declaration of Helsinki, as revised in 2013. All participants provided written informed consent before any study procedure.

Informed Consent

Not applicable.

Funding

This study did not receive specific funding from any public, commercial, or non-profit funding body. All laboratory costs were borne by the investigator and the host institution.

Data Sharing Statement

The de-identified dataset analysed in the present study is available from the corresponding author (Zainab Hudhi Farhood, zainabhadhi.bio@utq.edu.iq) upon reasonable written request, subject to local data-protection and ethical-review conditions stipulated by the Institutional Review Board of Al-Nasiriyah General/Turkish Hospital. Data-sharing requests will be reviewed by the corresponding author and the host institution and, where appropriate, a data-transfer agreement will be executed prior to release. No web-based public repository deposit is currently available because the dataset contains potentially identifiable clinical information from a single-centre Iraqi cohort; an anonymised, aggregated version may be deposited in an appropriate repository (e.g., Zenodo, Mendeley Data) after full publication, subject to ethical-review approval. The study protocol, statistical analysis plan, and biomarker assay protocols are also available from the corresponding author on request.

Conflict of Interest

The authors declare no competing interests.

Similarity Check

It was applied by Ithenticate[@].

Application of Artificial Intelligence (AI)

Not applicable.

Peer Review Process

It was performed.

References

1. Li Y, Choi H, Leung K, Jiang F, Graham DY, Leung WK. Global prevalence of *Helicobacter pylori* infection between 1980 and 2022: a systematic review and meta-analysis. Lancet Gastroenterol Hepatol. 2023;8(6):553–64.
2. Chen YC, Malfertheiner P, Yu HT, Kuo CL, Chang YY, Meng FT, et al. Global prevalence of *Helicobacter pylori* infection and incidence of gastric cancer between 1980 and 2022. Gastroenterology. 2024;166(4):605–19.
3. Saeed AY, Rashad BH, Ali BN, Sulaivany AH, Ibrahim KS. *Helicobacter pylori* infection: prevalence, risk factors, and treatment efficacy in symptomatic patients in Zakho City, Kurdistan Region, Iraq. Cureus. 2024;16(11):e73873.
4. Naqid IA, Al-Brefkani AMT, Hussein NR. A study of prevalence and risk factors for *Helicobacter pylori* infection among patients in Duhok city, Iraq. Arch Razi Inst. 2024;79(2):272–8.
5. Alsulaimany FAS, Awan ZA, Almohamady AM, Koumu MI, Yaghmoor BE, Elhady SS, et al. Prevalence of *Helicobacter pylori* infection and diagnostic methods in the Middle East and North Africa region. Medicina (Kaunas). 2020;56(4):169.
6. Gaonkar A, Zahiruddin QS, Shabil M, Menon SV, Kaur M, et al. Association of *Helicobacter pylori* infection and risk of dyslipidemia: a systematic review and meta-analysis. JGH Open. 2025;9(3):e70128.
7. Sun L, Zheng H, Qiu M, Hao S, Liu X, Zhu X, et al. *Helicobacter pylori* infection and risk of cardiovascular disease. Helicobacter. 2023;28(3):e12967.
8. Azami M, Baradaran HR, Dehghanbanadaki H, Kohnepoushi P, Saed L, Moradkhani A, et al. Association of *Helicobacter pylori* infection with the risk of metabolic syndrome and insulin resistance: an updated systematic review and meta-analysis. Diabetol Metab Syndr. 2021;13(1):145.
9. Niu Q, Zhu J, Yu X, Feng T, Ji H, Li Y, et al. Glucolipid metabolic disorders and *Helicobacter pylori* infection. Helicobacter. 2025;30(4):e70153.
10. Tegtmeyer N, Wessler S, Necchi V, Rohde M, Harrer A, Rau TT, et al. *Helicobacter pylori* employs a unique basolateral type IV secretion mechanism for CagA delivery. Cell Host Microbe. 2017;22(4):552–60.
11. Ansari S, Yamaoka Y. *Helicobacter pylori* virulence factor cytotoxin-associated gene A

(CagA)-mediated gastric pathogenicity. Int J Mol Sci. 2020;21(19):7430.

12. Liu W, Tian J, Hui W, Kong W, Feng Y, Si J, et al. A retrospective study on signal pathways induced by virulent protein CagA of *Helicobacter pylori*. Front Cell Infect Microbiol. 2023;13:1062803.
13. Smael DO, Hawrami KAM, Mohammed AB. Investigation of new *Helicobacter pylori* variants among cagA-positive strains using MLST typing method in Iraq. Sci Rep. 2025;15:34243.
14. Xia X, Zhang L, Wu H, Chen F, Liu X, Xu H, et al. CagA+ *Helicobacter pylori*, not CagA– *Helicobacter pylori*, infection impairs endothelial function through exosomes-mediated ROS formation. Front Cardiovasc Med. 2022;9:881372.
15. Shamil-Cherri F, Al-Mayahi RA, Hashim KH. Association between the proinflammatory cytokine IL-17F and *Helicobacter pylori* infection in a sample of Iraqi patients. Int J Biomed. 2023;13(2):338–41.
16. Al-Baldawy AN, Al-Marsomy HD, Khaleel II. Correlation between *Helicobacter pylori* infection and the level of serum inflammatory markers. Iraqi J Med Sci. 2023;21(2):155–62.
17. Yang XT, Niu PQ, Li XF, Sun MM, Wei W, Chen YQ, et al. Differential cytokine expression in gastric tissues highlights *Helicobacter pylori*'s role in gastritis. Sci Rep. 2024;14:7613.
18. Suzuki H, Nishizawa T, Tsugawa H, Mogami S, Hibi T. *Helicobacter pylori* infection and oxidative stress. J Clin Biochem Nutr. 2024;76(1):11–20.
19. Han L, Shu X, Wang J. *Helicobacter pylori*-mediated oxidative stress and gastric diseases: a review. Front Microbiol. 2022;13:811258.
20. Smirnova OV, Sinyakov AA, Kasparov EV. The role of immunoglobulin G (IgG), IgA and IgE—antibodies against *Helicobacter pylori* in the development of oxidative stress in patients with chronic gastritis. Biomedicines. 2022;10(8):2053.
21. Aslan M, Nazligul Y, Horoz M, Bolukbas C, Bolukbas FF, Aksoy N, et al. Serum paraoxonase-1 activity in *Helicobacter pylori* infected subjects. Atherosclerosis. 2008;196(1):270–4.
22. Akbas HS, Basyigit S, Suleymanlar I, Kemaloglu D, Koc S, Davran F, et al. The assessment of carotid intima media thickness and serum paraoxonase-1 activity in *Helicobacter pylori* positive subjects. Lipids Health Dis. 2010;9:92.
23. Tamura A, Fujioka T, Nasu M. Relation of *Helicobacter pylori* infection to plasma vitamin B12, folic acid, and homocysteine levels in patients who underwent diagnostic coronary arteriography. Am J Gastroenterol. 2002;97(4):861–6.
24. Tatsuguchi A, Miyake K, Gudis K, Futagami S, Tsukui T, Wada K, et al. *Helicobacter pylori* eradication lowers serum homocysteine level in patients without gastric atrophy. World J Gastroenterol. 2014;20(40):14823–8.
25. Dierkes J, Ebert M, Malfertheiner P, Luley C. *Helicobacter pylori* infection, vitamin B12 and homocysteine. A review. Dig Dis. 2003;21(3):237–44.
26. Yang YJ, Sheu BS, Yang HB, Lu CC, Chuang CC. Eradication of *Helicobacter pylori* increases adiponectin and decreases TNF-α in gastric mucosa of asymptomatic adults. Helicobacter. 2014;19(2):91–8.
27. Ozkan S, Sayin NC, Akbas H, Inan G, Yildiz F. Impact of *Helicobacter pylori* eradication on circulating adiponectin in humans. Helicobacter. 2013;18(3):225–9.
28. Vasile VC, Meeusen JW, Medina Inojosa JR, Donato LJ, Scott CG, Hyun MS, et al. Ceramide scores predict cardiovascular risk in the community. Arterioscler Thromb Vasc Biol. 2021;41(4):1558–69.
29. Hilvo M, Meikle PJ, Pedersen ER, Tell GS, Dhar I, Brenner H, et al. Development and validation of a ceramide- and phospholipid-based cardiovascular risk estimation score for coronary artery disease patients (CERT2). Eur Heart J. 2020;41(3):371–80.
30. Papazoglou AS, Stalikas N, Moysidis DV, Otountzidis N, Kartas A, Karagiannidis E, et al. CERT2 ceramide- and phospholipid-based risk score and major adverse cardiovascular events: a systematic review and meta-analysis. Atherosclerosis. 2022;345:34–42.
31. Peters L, Kuebler WM, Simmons S. Sphingolipids in atherosclerosis: chimeras in structure and function. Int J Mol Sci. 2022;23(19):11948.
32. Piccoli M, Cirillo F, Ghiroldi A, Tomasi M, Anastasia L, Coviello S, et al. Sphingolipids and atherosclerosis: the dual role of ceramide and sphingosine-1-phosphate. Antioxidants (Basel). 2023;12(1):143.
33. Mohammed ZJ, Rasool KH, Ahmed MA. Relationship between *Helicobacter pylori* infections and vitamin D level and lipid profile in some obese Iraqi women. Caspian J Environ Sci. 2021;19(5):801–7.
34. Mohammed AA, Ghadhban JM. Association between *Helicobacter pylori* virulence genes

UreA and CagA with histopathological changes in gastroduodenal disease. Iraqi J Med Sci. 2024;22(2):241–9.

35. von Elm E, Altman DG, Egger M, Pocock SJ, Gøtzsche PC, Vandenbroucke JP, et al. The Strengthening the Reporting of Observational Studies in Epidemiology (STROBE) statement: guidelines for reporting observational studies. Ann Intern Med. 2007;147(8):573–7.
36. Izhari MA, Al Mutawa OA, Mahzari A, Alqahtani AS, Hadadi AS, Hindi AAA, et al. *Helicobacter pylori* (*H. pylori*) infection-associated dyslipidemia in the Asir Region of Saudi Arabia. Life (Basel). 2023;13(11):2206.
37. Svedlund J, Sjödin I, Dotevall G. GSRS—a clinical rating scale for gastrointestinal symptoms in patients with irritable bowel syndrome and peptic ulcer disease. Dig Dis Sci. 1988;33(2):129–34.
38. Schröder H, Fitó M, Estruch R, Martínez-González MA, Corella D, Salas-Salvadó J, et al. A short screener is valid for assessing Mediterranean diet adherence among older Spanish men and women. J Nutr. 2011;141(6):1140–5.
39. Helou K, El Helou N, Mahfouz M, Mahfouz Y, Salameh P, Harmouche-Karaki M. Validity and reliability of an adapted Arabic version of the long international physical activity questionnaire. BMC Public Health. 2017;17:693.
40. Friedewald WT, Levy RI, Fredrickson DS. Estimation of the concentration of low-density lipoprotein cholesterol in plasma, without use of the preparative ultracentrifuge. Clin Chem. 1972;18(6):499–502.
41. Inker LA, Eneanya ND, Coresh J, Tighiouart H, Wang D, Sang Y, et al. New creatinine- and cystatin C-based equations to estimate GFR without race. N Engl J Med. 2021;385(19):1737–49.
42. Hirano T, Ito Y, Saegusa H, Yoshino G. A novel and simple method for quantification of small, dense LDL. J Lipid Res. 2003;44(11):2193–201.
43. Holvoet P, Macy E, Landeloos M, Jones D, Jenny NS, Van de Werf F, et al. Analytical performance and diagnostic accuracy of immunometric assays for the measurement of circulating oxidized LDL. Clin Chem. 2006;52(4):760–4.
44. Erel O. A novel automated direct measurement method for total antioxidant capacity using a new generation, more stable ABTS radical cation. Clin Biochem. 2004;37(4):277–85.
45. Erel O. A new automated colorimetric method for measuring total oxidant status. Clin Biochem. 2005;38(12):1103–11.
46. Folch J, Lees M, Sloane Stanley GH. A simple method for the isolation and purification of total lipides from animal tissues. J Biol Chem. 1957;226(1):497–509.
47. Pang Z, Chong J, Zhou G, de Lima Morais DA, Chang L, Barrette M, et al. MetaboAnalyst 5.0: narrowing the gap between raw spectra and functional insights. Nucleic Acids Res. 2021;49(W1):W388–96.
48. Dobiásová M, Frohlich J. The plasma parameter log (TG/HDL-C) as an atherogenic index: correlation with lipoprotein particle size and esterification rate in apoB-lipoprotein-depleted plasma (FERHDL). Clin Biochem. 2001;34(7):583–8.
49. DeLong ER, DeLong DM, Clarke-Pearson DL. Comparing the areas under two or more correlated receiver operating characteristic curves: a nonparametric approach. Biometrics. 1988;44(3):837–45.
50. Youden WJ. Index for rating diagnostic tests. Cancer. 1950;3(1):32–5.
51. Friedman J, Hastie T, Tibshirani R. Regularization paths for generalized linear models via coordinate descent. J Stat Softw. 2010;33(1):1–22.
52. Preacher KJ, Hayes AF. Asymptotic and resampling strategies for assessing and comparing indirect effects in multiple mediator models. Behav Res Methods. 2008;40(3):879–91.
53. Wang Z, Wang W, Gong R, Yao H, Fan M, Zeng J, et al. Eradication of *Helicobacter pylori* alleviates lipid metabolism deterioration: a large-cohort propensity score-matched analysis. Lipids Health Dis. 2022;21(1):34.
54. Kim TJ, Lee H, Kang M, Kim JE, Choi YH, Min YW, et al. *Helicobacter pylori* is associated with dyslipidemia but not with other risk factors of cardiovascular disease. Sci Rep. 2016;6:38015.
55. Aslan M, Horoz M, Nazligul Y, Bolukbas C, Bolukbas FF, Selek S, et al. The effect on serum myeloperoxidase activity and oxidative status of eradication treatment in patients *Helicobacter pylori* infected. Clin Biochem. 2011;44(13):1105–9.
56. Mackness M, Mackness B. Paraoxonase 1 and atherosclerosis. Front Cardiovasc Med. 2023;10:1065967.
57. Aydemir S, Bayraktaroglu T, Sert M, Sokmen C, Atmaca H, Mungan G, et al. The effect of *Helicobacter pylori* on insulin resistance. Dig Dis Sci. 2005;50(11):2090–3.

58. Summers SA, Chaurasia B, Holland WL. Metabolic messengers: ceramides. Nat Metab. 2019;1(11):1051–8.

59. Tsukanov VV, Smirnova OV, Kasparov EV, Sinyakov AA, Vasyutin AV, Tonkikh JL, et al. Dynamics of oxidative stress in *Helicobacter pylori*-positive patients with atrophic body gastritis and various stages of gastric cancer. Diagnostics (Basel). 2022;12(5):1203. doi: 10.3390/diagnostics12051203.